Functional Analysis of Pseudorabies Virus Genes

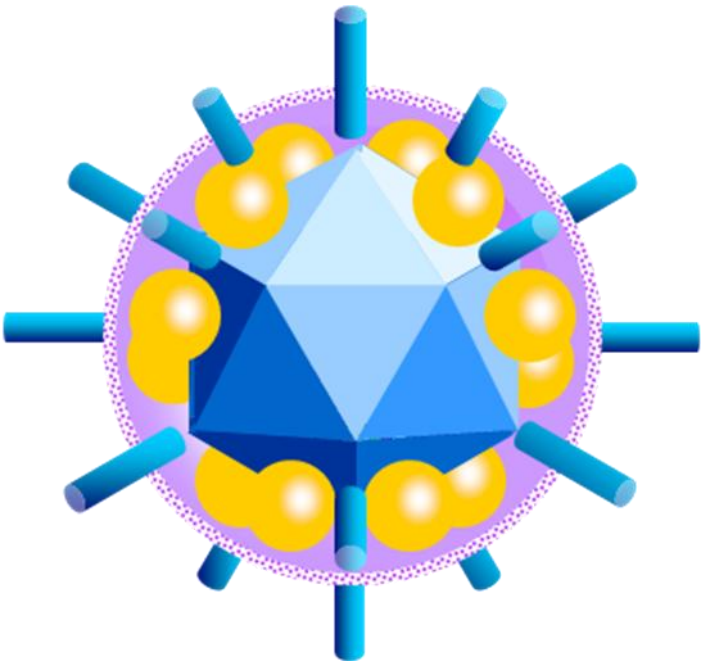

PhD Thesis

Dóra Tombácz

Supervisor: Zsolt Boldogkői

Department of Medical Biology

University of Szeged

Szeged, Hungary

2010

LIST OF PUBLICATIONS

FULL PAPERS DIRECTLY RELATED TO THE SUBJECT OF THE THESIS

I. Tombácz D, Tóth JS, Petrovszki P, Boldogkői, Z: Whole-genome analysis of pseudorabies virus gene expression by real-time quantitative RT-PCR assay. ***BMC Genomics*** 2009, **10**:491. IF: 3.926

II. Boldogkői Z, Bálint K, Awatramani GB, Balya D, Busskamp V, Viney TJ, Lagali PS, Duebel J, Pásti E, **Tombácz D**, Tóth JS, Takács IF, Scherf BG, Roska B: Genetically timed, Activity sensor and Rainbow transsynaptic viral tools. ***Nature Methods*** 2009, 6, 127 - 130

IF: 13.651

III. Prorok J, Kovács PP, Kristóf AA, Nagy N, **Tombácz D**, Tóth SJ, Ördög B, Jost N, Virágh L, Papp GJ, Varró A, Tóth A, Boldogkői Z: Herpesvirus-mediated delivery of a genetically encoded fluorescent Ca2+ sensor to primary adult canine cardiomyocytes. ***J Biomed Biotech*** 2009, 361795

IF: 2.563

IV. Rezek Ö, Boldogkői Z, **Tombácz D**, Kővágó C, Gerendai I, Palkovits M, Tóth IE: Location of parotid preganglionic neurons in the inferior salivatory nucleus and its relation to the superior salivatory nucleus of rat. Transneuronal labeling by pseudorabies viruses. ***Neurosci Lett*** 2008, 440(3): 265-269.

IF: 2.200

FULL PAPERS NOT RELATED TO THE SUBJECT OF THE THESIS

I. Márton G, **Tombácz D,** Tóth JS, Szabó A, Boldogkői Z, Dénes, Á, Hornyák Á, Nógrádi A: *In vivo* infection of human embryonic spinal cord neurons prior to transplantation into adult mouse cord， ***BMC Neuroscience*** 2010, *conditionally accepted for publication*
IF: 2.850

CUMMULATIVE IF: 25.190

ABSTRACTS RELATED TO THE SUBJECT OF THE THESIS

6. Tombácz D, Tóth JS, Petrovszki P, Boldogkői Z: Transcriptional analysis of Aujeszky's disease virus by Real-Time RT-PCR. ***Acta Microbiol Immunol Hung*** 2009, 56, 103.

5. Tóth JS, **Tombácz D**, Petrovszki P, Boldogkői Z: Regulatory function or transcriptional noise? – Antisense RNS sin Aujeszky's disease virus. ***Acta Microbiol Immunol Hung*** 2009, 56, 104.

4. Petrovszki P, **Tombácz D**, Tóth JS, Boldogkői Z: Activity sensor-expressing Aujeszky's disease viruses for neural circuit analysis. ***Acta Microbiol Immunol Hung*** 2009, 56, 81.

3. Tombácz D, Tóth JS, Boldogkői Z: Whole-genome analysis of pseudorabies virus by Real-Time RT-PCR. ***Acta Microbiol Immunol Hung*** 2009, 56, 253.

2. Márton G, **Tombácz D**, Tóth J, Szabó A, Boldogkői Z, Nógrádi A: Inhibition of pseudorabies virus spreading in the nervous system: effects of fluorescent tracers. ***Clin. Neurosci*** 2007, 61: 1, 43-44.

1. Tombácz D, Pásti E, Takács I, Bálint K, Roska B, Tóth J , Boldogkői Z: Development of pseudorabies virus-based transsynaptic gene delivery vectors**.** ***Acta Microbiol Immunol Hung*** 2007, 54, 134-135.

ORAL PRESENTATIONS

7. Tombácz D, Tóth JS, Boldogkői Z: Whole-genome analysis of pseudorabies virus by Real-Time RT-PCR. 2nd CEFORM Central European Forum for Microbiology, 2009, Keszthely, Hungary

6. Tóth JS, **Tombacz D**, Bálint K, Roska B, Boldogkoi Z: Genetically modified pseudorabies viruses for neural circuit analysis. I. International Student Medical Congress, 2009, Kosice, Slovakia

5. Tombácz D, Boldogkői Z: Az Aujeszky-féle vírus összgenom analízise Real-Time RT-PCR-ral. „Genetikai Műhelyek Magyarországon" - VIII. Genetikai minikonferencia, 2009, Szeged, Hungary

4. Tóth J, **Tombácz D**, Petrovszki P, Boldogkői Z: Az Aujeszky-féle vírus transzkriptom vizsgálata kvantitatív RT-PCR-ral VIII. Magyar Genetikai Kongresszus / XV. Sejt- és Fejlődésbiológiai Napok, 2009, Nyíregyháza, Hungary

3. Nagy V, **Tombácz D**, Boldogkői Z: Az Aujeszky-féle vírus genom transzkripciós analízise. XXIX. Biológia OTDK, 2009, Veszprém, Hungary

2. Petrovszki P, **Tombácz D**, Tóth JS, Boldogkői Z: Neuronhálózatok aktivitásának vizsgálata rekombináns Aujeszky-féle vírusokkal. Genetikai Minikonferencia, 2008, Szeged, Hungary

1. Tombácz D, Tóth JS, Petrovszki P, Boldogkői Z: Az Aujeszky-féle vírus genom transzkripciós analízise real-time RT-PCR technikával. A Magyar Mikrobiológiai Társaság 2008. évi Nagygyűlése, 2008, Keszthely, Hungary

POSTER PRESENTATIONS

12. Tombácz D, Tóth JS, Takács IF, Boldogkői Z: Global analysis of pseudorabies virus gene expression by RT-PCR. Advances In Genomics Symposium, 2010, Ghent, Belgium

11. Ferecskó AS, Boldogkői Z, **Tombácz D**, Ördög B, Hirase H, Tiesinga P , Sík A: Development of a novel pseudorabies virus-based method for monosynaptic neuronal network tracing. IBRO International Workshop, 2010, Pécs, Hungary

10. Marton G, **Tombacz D**, Toth J, SzaboA, Boldogkői Z, Nógrádi A: Effect of the fluorescent tracer Fast Blue on the Pseudorabies virus infection. Frontiers in system neuroscience, 2009, Chicago, IL, USA

9. Tombácz D, Tóth JS, Petrovszki P, Boldogkői Z: Real-time RT-PCR Profiling of Global mRNA Transcription from Pseudorabies Virus Genome. 34th International Herpesvirus Workshop, 2009, Ithaca, NY, USA

8. Petrovszki P, **Tombácz D**, Tóth JS, Sík A, Bálint K, Roska B, Boldogkői Z: Fluorescent calcium sensor expressing pseudorabies viruses for the study of neural circuits. HFSP 20th Anniversary and 9th Awardees Meeting, 2009, Tokyo, Japan

7. Márton G., **Tombácz D**, Tóth J, Szabó A, **Boldogkői Z**, Nógrádi A: Effect of the fluorescent tracer Fast Blue on the Pseudorabies virus infection, A Magyar Idegtudományi Társaság XII. Konferenciája, 2009, Budapest, Hungary

6. Prorok J, Tóth A, Iost N, Kovács PP, Kristóf AA, **Tombácz D**, Tóth J, Ördög B, Virág L, Papp JG, Varró A, Boldogkői Z: Herpesvirus-mediated delivery of genetically encoded fluorescent Ca2+ sensor to adult canine cardiomyocytes. 32nd Meeting of the European Working Group on Cardiac and Cellular Electrophysiology, 2008, Madrid, Spain

5. Tombácz D, Tóth JS, Bálint K, Roska B, Boldogkői Z: Activity sensor expressing pseudorabies viruses for the study of neural circuits. 33rd Annual International Herpesvirus Workshop, 2008, Estoril, Portugal

4.Tóth JS, **Tombácz D**, Petrovszki P, Boldogkői Z: Genome-wide antisense transcription in pseudorabies virus. 33rd Annual International Herpesvirus Workshop, 2008, Estoril, Portugal

3. Tóth JS, **Tombácz D**, Petrovszki P, Boldogkői Z: Szabályozás, vagy transzkripciós zaj? – Antiszensz RNS-ek az Aujeszky-féle vírusnál. A Magyar Mikrobiológiai Társaság 2008. évi Nagygyűlése, 2008, Keszthely, Hungary

2. Petrovszki P, **Tombácz D**, Tóth JS, Boldogkői Z: Aktivitás szenzort kifejező Aujeszky-féle vírusok ideghálózatok térképezésére. A Magyar Mikrobiológiai Társaság 2008. évi Nagygyűlése, 2008, Keszthely, Hungary

1. Tombácz D, Pásti E, Takács I, Bálint K, Roska B, Tóth J, Boldogkői Z: Development of pseudorabies virus-based transsynaptic gene delivery vectors. 15th International Congress of Hungarian Society for Mirobiology

CONTENTS

LIST OF ABBREVIATIONS

AS-RNA	Antisense RNA
ASP	Putative Antisense promoter
BDR	Bartha DsRed
CFP	Cyan fluorescent protein
CHX	Cycloheximide
CNS	Central nervous system
Ct	Threshold cycle
DMEM	Dulbecco's Modified Eagle Medium
E	Early
E	Efficiency
EDTA	Ethylene diamine tetra-acetic acid
EHV	Equine herpesvirus
ep0	Early protein 0 gene
EtBr	Ethidium bromide
FP	Fluorescent protein
FRET	Fluorescence resonance energy transfer
GCV (MP, TP)	Ganciclovir (monophosphate, triphosphate)
GFP	Green fluorescent protein
HSV (-1, -2)	Herpes simplex virus (type-1 and type-2)
IE	Immediate early
IR	Inverted repeat
ISN	Inferior salivatory nucleus
KO	Knock-out
L	Late
LAP	Latency-associated promoter
LAT	Latency associated transcript
LLT	Long latency transcript
MARCKS[2]	Myristoylated alanine-rich C-kinase substrate
memGFP	Membrane-targeted green fluorescent protein
miRNA	micro RNA
mRFP	Monomeric red fluorescent protein
MOI	Multiplicity of infection

NC	Non-coding
ORF	Open reading frame
ORI	Origin of replication
PAA	Phosphonoacetic acid
PAC element	Packaged and cleavaged
PBS	Phosphate buffered saline
PCR	Polymerase chain reaction
piRNA	piwi-interacting RNA
PK-15	Porcine kidney 15
PRV	Pseudorabies virus
PRV –Ba	Bartha strain of PRV
PRV– Ka	Kaplan strain of PRV
r	Pearson's correlation coefficient
R	Relative expression ratio
R_a	Rates of change
R_Δ	Net increase of the relative expression ratios between two time points
RE	Restriction endonuclease
$R_{i\text{-}CHX}$	Inhibitory effect of CHX on the gene expression
$R_{i\text{-}PAA}$	Inhibitory effect of PAA treatment on the gene expression
RR	Ribonucleotide reductase
RT	Reverse transcription
RT^2-PCR	Reverse transcription Real-Time PCR
SDS	Sodium dodecyl sulfate
SE	Standard error
siRNA	Small interfering RNA
SSN	Superior salivatory nucleus
TBE	Tris-borate-EDTA buffer
TFP	Teal fluorescent protein
Tm	Melting temperature
TR	Terminal repeat
UT	Untreated (non treated)
VHS	Virion host shutoff
VZV	Varicella zoster virus
wt	wild-type

INTRODUCTION

Pseudorabies virus

The pseudorabies virus (PRV; also called suid herpesvirus type 1, or Aujeszky's disease virus) belongs to the subfamily of *Alphaherpesvirinae* (also called neurotropic herpesviruses) of *Herpesviridae* family. PRV, together its close relatives, the Varicella-zoster virus, the bovine herpesviruses and equine herpesviruses are the members of the *Varicellovirus* genus. In spite of its name, PRV has no relationship to rabies virus; the name came from the symptoms similar to those of rabies caused in susceptible animals [1]. PRV is an important pathogen of swine, causing Aujeszky's disease [2]. Albeit, great efforts have been taken to eradicate PRV in Europe and in the United States, it still causes economic losses in many countries worldwide [3]. This virus has an extremely broad host spectrum including, among others, rodents, ungulates and carnivorous animals. However, human, higher primates and horses are resistant to PRV infection [1]. PRV can exhibit two alternative infectious pathways; it can infect cell in a lytic way causing cytopathic effects and producing new viral particles, or it can establish latency in the sensory ganglia [3].

Due to the significant homology among the members of neurotropic herpesviruses, information derived from the PRV studies provides a powerful opportunity for comparative molecular virology [4]. PRV is a frequently used model organism for studies in pathogenesis and molecular biology of herpesviruses. Furthermore, this virus is widely utilized as a neural circuit tracer [5, 6 and 7] in neurobiology, and it has also reported to serve as a suitable too for gene delivery to various cells [8, 9].

Like all the member of herpesviruses, the PRV contains a large linear double-stranded (ds) DNA genome (it is 142 kb in length with a G+C content of 74%) and has 70 protein coding genes. The virus genome consists of a unique long (U_L) and a unique short (U_S) region flanked by inverted repeat (IR) sequences. About half of the gene products are structural components of the virion. The mature virion, consists of four main morphologically distinct structural elements (Figure 1.): a central core containing the virus genome, an icosahedral capsid (forming the nucleocapsid with the DNA), a tegument layer (protein matrix) and an envelope (host cell lipid membrane with viral glycoprotein spikes) [3].

PRV genome has been reconstructed from sequences of six different strains (Kaplan, Becker, Rice, Indiana-Funkhauser, NIA-3, and TNL) [10].

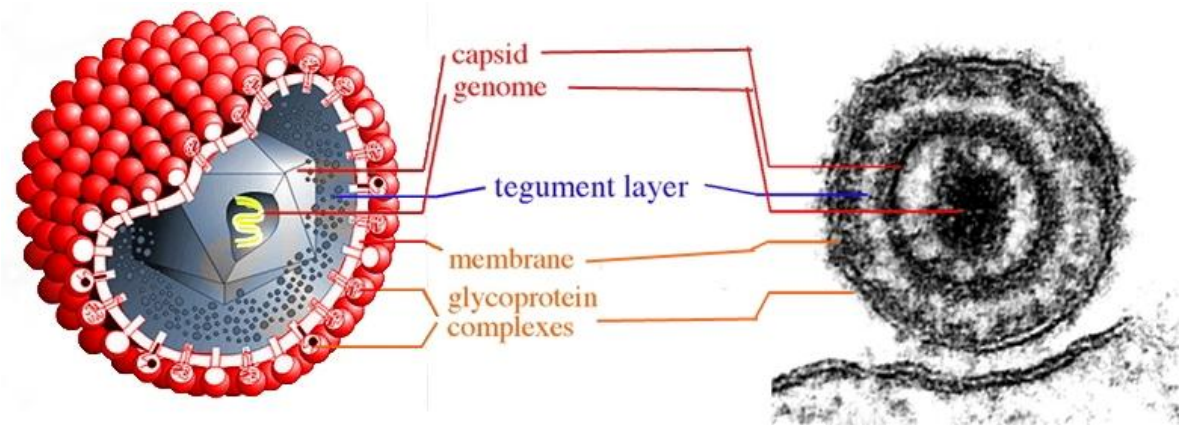

Figure 1. A schematic drawing and an electron microscope image of the PRV virion.

The PRV genome and the genes

Herpesvirus gene expression

The expression of PRV genes is mainly regulated at the level of transcription. The genes of α-herpesviruses are divided into three major temporal classes: (immediate-early, IE or α; early, E or β, and late, L or γ), which are regulated in a coordinated, cascade-like fashion [11 and 12]. First the IE genes are expressed, independently of *de novo* protein synthesis from the virus. They are regulatory genes. PRV contains a single IE gene, the *ie180* gene [homologous to herpes simplex virus (HSV) ICP4 gene], which is transactivator of the expression of the entire PRV genes. Early genes are mainly involved in DNA synthesis of the virus. On a finer scale, the E genes can be subdivided into β1 (E) and β2 (E/L) genes. Finally, the late genes are expressed; they mainly encode the structural elements of the virus. Blockers of DNA replication inhibit the expression of L genes to a larger extent than E genes expression. The transcription of the L genes is partially (γ1, leaky L genes) or completely (γ2, true L genes) dependent on the viral DNA synthesis [3].

HSV expresses 5 IE genes: *icp0*, *icp4*, *icp22*, *icp27* and *icp47*, while PRV encodes a single IE gene, the *ie180* gene. The *ep0* (homologous to the homolog of HSV *icp0* gene; [13] and *ul54* (homologous to the *icp27* of HSV; [14]) are expressed proteins in E kinetics in PRV, and this virus lacks the *icp47* gene. There is no consensus as to whether the US1 protein (Rsp40; homologous to HSV ICP22) is expressed in the IE [15] or the E kinetics [16].

Infection of cells by herpesviruses can lead to either lytic (productive) or latent infection [3]. In productive infection, the entire transcription machinery of the herpesvirus is initiated, and the progress of infection leads to the production of new virus particles, meanwhile exerting strong cytotoxic effects. Contrary to productive infection, during the latent stage, a limited

segment (latency-associated transcript; LAT region) of the herpesvirus genome is transcriptionally active [17], no new virions are produced and the cells survive the infection. The LATs are transcribed from the opposite strand of EP0 gene [3]. A characteristic feature of the organization of the herpesvirus genome is so called nested localization of genes which produce 3'-coterminal transcripts. Nested genes form convergent (Figure 2.) or divergent clusters on the PRV genome.

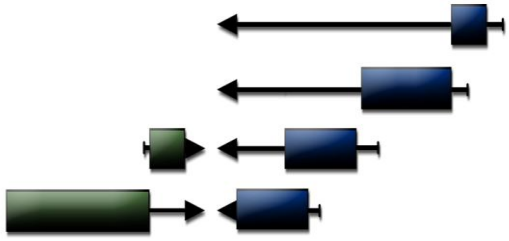

Figure 2. Schematic illustration of oppositely oriented nested gene clusters *with common 3' ends. Arrows represents the PRV genes and their orientations, while the rectangules represents the protein coding sequences.*

ICP27 has been reported to affect the use of certain internal polyA signals, resulting in differential transcript lengths throughout the life cycle of the virus [18, 19]. The read-through of transcription of the nested genes is regulated by the ICP27 protein [18]. In neurotropic herpesviruses only a few gene was found to be spliced. PRV contains two spliced (US1 and LAT) and a putative spliced transcript (UL15). Their homologs are also spliced in HSV [3].

Traditionally, herpesvirus gene expression has been analyzed using Northern blot technique, ribonuclease protection assay, and end-point RT-PCR analysis. Nevertheless, these techniques have several disadvantages. For example, Northern blotting is time-consuming and labor-intensive, allows only semiquantitative determination of the mRNA level and it is looking at one or a small number of genes at the same time. Moreover, hybridization-based membrane arrays profile changes in a nonlinear fashion, tending to overemphasize large alterations, and they are insensitive to smaller variations. Ribonuclease protection assay-based methods require the use of polyacrylamide gel electrophoresis and typically utilize radioactively labeled probes. The limitations of endpoint PCR technique are the low sensitivity and resolution, the poor precision, and the variable endpoints between samples. The endpoint detection is very time consuming and need for post PCR processing (ethidium bromide for staining which is not very quantitative).

Over the past decade, DNA chip techniques have revolutionized practically all disciplines of molecular biology, including herpesvirus research. Contrary to the traditional methods, microarray analysis is applicable for the parallel analysis of a large set of gene product, and even whole genomes. The disadvantage of DNA chip technology is associated with the uncertain quality control: it is impossible to assess the identity of DNA immobilized on any

microarray. Further, fluorescence technology, which is the most commonly used detection method for array readouts is reproducible, but is limited in sensitivity and there are many artifacts associated with image and data analysis. Real-time RT-PCR (RT^2-PCR) is an alternative to microarray techniques for the analysis of transcription from multiple genes. An advantage of RT-PCR is its high sensitivity compared to other high-throughput assays. Furthermore, the RT-PCR technique offers numerous other advantages, such as reproducible quantitation of DNA copies and large dynamic range. Furthermore, in RT^2-PCR various controls can be included to ensure accuracy, such as a loading control to verify equal cDNA loading, a no-primer control to prove a measure of non-amplification-related background, a no-template control to screen for possible contamination of reagents or false amplification products, and a no-RT control with confirm the absence of DNA contamination. In contrast to DNA chip techniques, in RT-PCR the parameters for each gene can be individually optimized. Moreover, the identity of PCR products can be confirmed through melting curve analysis, restriction endonuclease analysis, or DNA sequencing. In fact, real-time PCR is often used to verify gene expression data obtained by microarrays. Nevertheless, considerable pitfalls may be associated with this technique. The major disadvantage of real-time RT-PCR compared to microarray techniques is the higher cost and labor-consuming work for a large number of samples. Another disadvantage of real-time PCR as compared with blotting techniques is that only the accumulation, but not the size of the transcripts can be monitored. Microarray techniques have recently been applied to investigate herpesvirus gene expression [20, 21, 22 and 23]; to analyze the effects of the deletion of particular viral genes or of the specific experimental conditions on whole-genome viral gene expression [24, 25, and 26]; and to analyze the impact of virus infection on the expression of cellular genes [27, 28, 29 and 30].

The kinetic properties of PRV genes have been characterized by traditional methods, but many of its genes have not yet been studied at all. Flori and colleagues [30] investigated the dialog between PRV and epithelial cells, but obtained poor resolution for viral transcripts that did not provide conclusive data on the temporal expression of the PRV genes. To date, RT^2-PCR has not been frequently utilized in herpesvirus research for global gene expression analysis. With this technique Oster and Höllsberg [31] performed an expression study of 35 genes of human herpesvirus 6B, a β-herpesvirus, and Dittmer and co-workers [32] carried out a whole-genome profiling of the rhesus monkey rhadinovirus, a γ-herpesvirus. As far as we are aware, no genome-wide expression data obtained by RT^2-PCR have been published so far on α-herpesviruses.

PRV genes

The PRV has 70 different genes. PRV has two copies of *ie180* and *us1* genes because these genes are localized in the repeat regions of the virus. The gene nomenclature is derived from the location order of HSV genes on the viral DNA [3]. The genome of PRV and HSV are colinear with each other, except for a large inversion between the *ul46* and *ul26.5* genes, in the U_L region of PRV. Some HSV genes are not found in PRV, while the *orf1*, *orf1.2* and *ul3.5* genes of PRV are not found in HSV [10].

(1) The early protein 0 (ep0) gene

As its name implies, *ep0* is expressed in the early phase of infection. Although, the function of the *ep0* gene is not clear, an *ep0* negative mutant virus produces lower titer and smaller plaques compared to the wild-type (wt) PRV [33]. The *ep0* is a transactivator gene; it has been shown to facilitate the expression of the *ie180, ul23* and *us4* PRV genes and several other genes in HSV and VZV. The *ep0* gene overlaps with the oppositely transcribed latency-associated transcript (LLT). The *ep0* deleted PRV mutants are attenuated in neonatal piglets and other animals [34].

The members of the *Alpha-*, *Beta-*, and *Gammaherpesvirinae* subfamilies have 40 conserved genes (core genes) in the U_L region, which encode proteins involved in the replication. Phylogenetic analysis of herpesviruses suggests that an ancestral virus contributed the 40 core genes to modern herpesviruses [35]. Other protein coding genes (*ul19, ul35, ul38, ul18, ul6, ul25*) of the U_L region play a role in capsid formation. The tegument layer consist of at least fifteen viral proteins (encoded by the *ul51, ul49, ul48, ul47, ul46, ul31, ul36, ul37, ul41, ul21, ul16, ul13, ul11, us3* and *us2* genes) and actin from the host cell [36]. Tegument proteins play essential roles in virus entry and virion morphogenesis [37]. After the fusion of the envelope with the infected cell membrane, these proteins enter the cell together with the capsid and assist to taking over the control of host cell. The α-TIF protein (also known as VP16 protein) encoded by the *ul48* gene, is one of the tegument proteins, and is involved in triggering the IE gene expression.

(2) Virion host shutoff (VHS, ul41) gene

Virion host shut-off (VHS) protein, the product of the *ul41* gene of herpesviruses, is responsible for the rapid shutoff of host cellular protein synthesis after virus entry into the cells [38]. VHS protein is a ribonuclease (RNase) [39]. During the lytic infection period, it negatively regulates the half-life both of cellular and viral mRNAs [40]. Approximately 200 copies of this polypeptide within the tegument of the infecting virus [41] lead to nonspecific

cytoplasmic degradation of host cell mRNAs and viral transcripts, as well as, polysomal disaggregation [42]. The coordinated regulation of the different temporal classes of viral genes is also accomplished in part through the action of the VHS protein [43]. While, the VHS polypeptide degrades both viral and cellular transcripts very quickly by an unknown mechanism, it does not cause degradation of tRNAs and rRNAs [44]. VHS protein mediates this, primary (early) stage of the shutoff phenomenon, which does not require newly synthesized proteins of the virus. The secondary (delayed) shutoff caused by the *ul54* gene requires the transcription of viral genes [45]. The role of the *ul54* gene is the shutoff of host protein synthesis.

The *vhs* gene is expressed at the late (leaky-late, γ1, or early-late) stage of HSV infection. This gene expresses two forms of the VHS protein, the 58 kDa polypeptide and the 59.5 kDa phosphoprotein (the latter is highly phosphorylated) [46]. During the late stage of the herpesvirus replication cycle, the VHS peptide forms a complex with the product of *ul48* gene, the α-TIF protein, which is the transcriptional activator of the virus. It modulates the VHS shutoff activity during infection [47].

VHS plays an essential and conserved role in the biology of infections of alphaherpesviruses, present in all of their genomes [3]. Sequence analysis of the members of the *Alphaherpesvirinae* subfamily (HSV-1, HSV-2, VZV, EHV and PRV) revealed that all of these neurotropic herpesviruses have a homolog of VHS, four conserved domains with 89% amino acid identity, but this conservation is absent in beta- and gamma-herpesviruses. Supporting this concept, the VHS-deleted herpesviruses have a reduced ability to replicate in the brain of the mouse [41]. The *ul41* gene is nonessential, since a VHS knockout virus retains its ability to grow in cell culture, however, deleted VHS function results in a five- to tenfold reduction of the virus in cultured cells. Several studies indicate that the VHS protein play an important role in the viral pathogenesis [43, 48, 49].

(3) The gE and the gI genes

The PRV genome encodes 16 glycoproteins which are localized in the membranes of the host cell as well as in the viral envelope. These proteins have functions in entry, egress and cell-to-cell spread of the virus and also promote the syncytia formation and control the immune response. Eleven of the 16 proteins are glycosylated (gB, gC, gD, gE, gG, gH, gI, gK, gL, gM, and gN) [50]. During entry, the gC, gB, gD, gH, and gL proteins are responsible for virion attachment to the infected cell surface and the fusion of the virion envelope with cell membrane. Several viral envelope glycoproteins have been shown to represent targets for host's immune defense [51].

The standard nomenclature of alpha-herpesvirus glycoproteins was adopted at the 18th International Herpesvirus Workshop in 1993. PRV glycoprotein E (gE) and glycoprotein I (gI) (encoded by the *us8* and *us7* genes, respectively) form non-covalently bound physical, hetero-oligomeric complexes which are conserved in α-herpesviruses and many functions attributed to them [52, 53, 54].

The US8 transcript of PRV is categorized as an early gene [55], while its homolog in HSV is described either as an early [56, 57] or as a late gene [58, 59]; so there is no consensus on this issue. The *us8* gene codes for the gE glycoprotein which plays an important role in direct cell-to-cell spread of the virus [54, 60, 61, 62 and 63]. The gE is also required for neurovirulence. This protein is dispensable for viral replication in tissue culture and infection. In cell cultures, the gE-deleted virus forms smaller plaques than the wild type. The domain mediating neurovirulence is encoded within the cytoplasmic tail of the gE protein [64]. Several studies suggest that the gE cytoplasmic tail interacts with the products of *ul49* gene (VP22 protein). This tegument protein also interacts with the glycoprotein M (gM, encoded by the *ul10* gene). The gE protein together with the gM and VP22, plays a role in the secondary envelopment of the virus during egress [65]. The cytoplasmic tail of gE is not required for the formation of a complex with glycoprotein (g)I. The gE gene of PRV is conserved among the neurotropic herpesviruses indicating the importance of this gene for these viruses. The *us7* gene of PRV encodes the viral glycoprotein gI. Our knowledge about the *us7* expression kinetics in PRV is very poor; its transcript was detected 6 hours post-infection at high MOI (multiplicity of infection) in porcine kidney–15 (PK-15) cells. Kinetic properties are not well characterized in HSV either (it is an early or a late gene; there is no general agreement on this issue).

The gI is not an essential protein for replication in tissue culture [66]. The gE/gI complex plays a role in anterograde spread of the virus from the peripheral nervous system to the central nervous system [54, 60-63]. Following the infection of the rat eye, the wild type virus replicates in retinal ganglion neurons and then spreads in an anterograde manner to all visual nuclei in the central nervous system (CNS) [67]. Contrary to the wt PRV, gE/gI mutant viruses replicate in the eye, but do not spread to the second-order neurons in CNS. Infection of olfactory nervous pathway, as well as trigeminal ganglia of swine with gE/gI-mutant PRV showed reduced neuronvirulence and defective anterograde spread in the CNS [54, 60-62]. In cell culture, the gI-deleted virus forms smaller plaques [62]. The gE and gI glycoproteins are not required for retrograde spreading [64]. Glycoprotein I homologs are found only in *Alphaherpesvirinae*.

(4) Thymidine kinase (TK) gene

Several enzymes encoded by the PRV genome are involved in the nucleotide metabolism. For example, PRV and also HSV contain the *ul23* (encoding the viral thymidine kinase, TK), the *ul50* (encoding dUTPase), *ul39* and *ul40* (encoding the large and small subunits of ribonucleotide reductase, RR1 and RR2, respectively). The *ul23* gene can only be found in the α- and γ-herpesvirus subfamilies. This enzyme has a key role in the replication of viral DNA; it catalyzes the phosphorylation of deoxythymidine which is an important step in the dTTP synthesis pathway. The TK gene is not essential for virus replication in cultured cells, but it is essential for the propagation in living animals: *UL23*-negative PRV mutants are not able to replicate in mice, rabbits or pigs [68, 69].

(5) Ribonucleotide reductase (RR) gene

The RR enzyme catalyzes the conversion of ribonucleotide diphosphates into deoxyribonucleotide diphosphates, which are raw materials for the DNA synthesis. The herpesvirus enzymes consist of two non-identical subunits. The RR subunits are encoded by the *ul39* (the large subunit, RR1) and *ul40* (the small subunit, RR2) genes. The *ul39* or *ul40* mutant PRV viruses are able to replicate in cell culture, while are severely attenuated in pigs and mice. The RR1 gene contains several highly conserved sequences [70].

Genomic sequences

(5) ASP (antisense promoter)

The putative antisense promoter (ASP) is located at the inverted repeat region of the PRV, therefore, it is represented in two copies. It has been suggested that the role of ASP is to control the expression of an antisense transcript called AST (antisense transcript), but it's precise function has not yet been elaborated. It has been earlier reported that even a point mutation in the ASP region (within the putative TATAA box of the promoter) results in a significant reduction of virulence in PRV [71].

(6) PAC (Package and cleavage)

The encapsidation of the PRV genome requires the cleavages of the replicated concatameric DNA into monomeric DNA segments followed by the packaging of these unit-length PRV DNA molecules into the empty capsids [72, 73]. Two conserved domains (the *pac1* and the *pac2*) at the ends of the linear herpesvirus genomes are necessary for the site-specific DNA-cleavage and packaging. While the *pac1* resides near the end of the TR (terminal repeat) and in the IR sequence (close to the U_L region), the *pac2* domain is located at the end of the U_L region.

(7) ORI (Origin of replication)

Three well-defined origins of replication have been found in PRV: two copies of *OriS* in the inverted repeats and an *OriL* mapped in the U_L region [15, 74].

(8) Neut region

The *Bam*HI8' fragment of PRV genome is located between the *ep0* and *ie180* genes, and contains contains several unique restriction sites. A mutation in several locations of this region is neutral; that is, it does not cause detectable decline in the virulence [71].

Antisense RNAs

During the past few years, the traditional view of RNA as a passive intermediary between DNA and protein has been changed, by the finding that the great majority of the mammalian genome is transcribed, and that an increasing number of antisense (AS) RNAs have been discovered in many species. The advances in understanding of the role of AS-RNAs altered the paradigms applied to gene regulation and function [75, 76].

Natural antisense transcripts (NATs) are RNAs that exhibit complementary sequences to other endogenous transcripts (they are complementary to protein coding genes). They are categorized into two goups, *cis* and *trans*. The *cis*-natural antisense transcripts, also known as overlapping AS-RNAs, have been intensely studying nowadays. They have been first described in prokaryotes, but they are common in viruses, bacteria, and eukaryotes [77]. The *cis*-overlapping AS-RNAs are transcribed from the opposite strands of the same DNA locus, whereas *trans*-encoded NATs (e.g. miRNAs) are transcribed from distant loci. [75]. The *cis*-NATs (>200 bases) [78] are supposed to exhibit a perfect complementarity to mRNAs and they overlap each other at least partially, by contrast the *trans*-NATs are small RNAs and they exhibit high, but imperfect complementarities between the sense and AS transcripts [79].

The antisense transcription in human was first described in 1981 [80]. Previous studies have estimated 1%–15% of human genes having antisense partners [75]. This ratio could be 22%, in *Drosophila melanogaster* and it is 10% in *Arabidopsis thaliana* [81, 82]. Transcription of long, *cis*-antisense transcripts is a common phenomenon in the mammalian genome [83]). Recently, the genome-wide studies revealed widespread NATs in eukaryotes (approximately 20-26% of the human genes form sense-antisense gene pairs and it is proposed that the gene regulation by AS transcripts may be much more common than previously thought. [79]). Furthermore, some sense-antisense gene pairs are conserved across species. In the 21st century, it has become evident that the large part of the genome (including introns and other intergenic sequences) is in fact expressed, often from both DNA strands and clearly in a developmentally regulated

manner [78]. Recent studies (based on whole-genome tiling arrays and cDNA cloning techniques) show that the majority of all eukaryotic genome from yeast to human are transcribed [84-87]. Whole transcriptome studies have shown that at least 80% of the human transcripts are exclusively associated with *cis*- non-coding RNAs (*cis*-NC-RNAs) [88].

It has been published [89] that *cis*-encoded antisense RNAs play a role in the downregulation of gene expression in prokaryotes. The NC transcripts of mammals have diverse biological functions, for example: controlling of transcription, proliferation or growth etc. [90]. These characteristic features suggest that NC-RNAs are even more widely expressed in eukaryotes than in prokaryotes. One of the functions of these RNAs appears to be as epigenetic regulators of the protein coding genes. The *cis*-AS-RNAs also frequently associated with the genomic imprinting in mammals, it has also been described that they directly modulate the gene expression and protein degradation as well as they have roles in organelle biogenesis and subcellular trafficking [91, 92, and 93]. The possible function of these transcripts in the formation of dsRNAs, which may be cleaved into small interfering RNAs (siRNAs), now is under investigation. Our view on the general role of RNAs has dramatically changed in the 1990s, by the discovery of RNA interference (RNAi), albeit it was originally been associated with exogenous siRNAs, it has become clear that higher-order organisms [94, 95] also produce endogenous siRNAs. In human, there are hundreds of siRNAs, as well as other small RNAs; at least 700 miRNAs, and millions of piRNAs (piRNAs form protein-RNA complexes with Piwi proteins and participate in gene silencing.) [93]. The endogenous siRNAs have recently been identified in *Drosophila* and in mammals are involved in post-transcription gene regulation, anti-viral defence, transposon silencing, chromatin remodelling, as well as, like the protein coding genes, these small RNAs can function either as mediator of various diseases [96, 97]. Another class of small NC-RNAs, the miRNAs is predicted to regulate al least one-third of all human genes [98].

Albeit, large number of studies have been published on AS-RNAs in various organisms [99-104], a little is known about "whole antisense transcription" of herpesviruses. Individual AS transcripts have been described in all the herpesvirus subfamilies. Zhang and colleagues found genome-wide antisense RNAs in a HCMV, which is a member of the *Betaherpesvirinae* subfamily, a distant relative of PRV [75]. It has been long known, that PRV expresses specific antisense RNAs, which are the latency-associated transcript (LAT), and the long latency transcripts (LLTs) oriented oppositely to *ep0* and *ie180* genes, respectively. These AS transcripts are considered to play roles in the latent state established in specific neurons by the virus, but certain level of expression has also been reported in other cell types [3].

Herpesviruses as neural circuit tracers

To understand the function of the brain, it is essential to know its structure and the connections between neurons [8]. Due to fact that the CNS consist of a network of enormous number of neurons it is practically impossible to track their connections without specifically labeling individual neurons or a small group of cells [8, 105]. Various circuit labeling methods were developed in the 1990s [8]. The non-viral techniques for mapping functional connections of neurons involve the inoculation of dyes or enzymes into a particular region of the brain. The tracing material is taken up from this area, by nerve terminals and transported along axons [106]. However, most of these traditional tracers are not or inefficiently transported to synaptically connected neurons. Hence, it is difficult to label multi-component neuronal pathways by these dyes. Therefore, multisynaptic viral tracers are inevitable tools in the analysis of neural pathways [1, 8]. Initially, wt and traditionally generated neurotropic viruses were used for this purpose. Nevertheless, the natural features of these circuit-tracing viruses impose severe limitations in tracing paradigms. Genetic engineering of these viruses offers a tool to get rid of their disadvantageous properties (e. g. cytotoxicity) and to equip them with novel characteristics lacking from their parent viruses [8].

In recent years PRV has become the most popular neurotropic herpesvirus for tracing studies, it has been used as a live tracer of the neural networks due to its propensity to infect synaptically connected neurons [3, 107]. PRV is suitable for delivering large foreign DNA fragments and mutated genomic sequences. These properties of PRV make it a useful tool for studies in the field of neuroscience.

PRVs expressing fluorescent proteins (FPs) are effective for labeling neurons in a functional neural network *in vitro* and also *in vivo*. In addition, it is possible to generate recombinant viruses expressing genetically encoded fluorescent Ca^{2+} indicators that report the activity of the infected cells.

Generally, the virulent PRV strains (e.g. NIA-3, PRV-Becker), which induce rapid, lethal inflammatory responses within 2-3 days after infection, are not suitable tracer, because the injected animals die before the target neurons become infected [1].

One of the most widely used virus is an attenuated PRV strain (PRV-Bartha, PRV-Ba, generated in 1961), which induces reduced inflammatory responses and contrary to the wt PRVs, it spreads in an exclusively retrograde manner [108]. Recombinant PRV-Ba strains are also employed as retrograde transsynaptical tracers. This virus is also widely used in Europe as a live vaccine against Aujeszky's disease [2]. It was generated by traditional mutagenesis and selected on the basis of its plaque morphology (it produces small plaques; [109]). PRV-Ba has

several recognized mutations, including a deletion in the unique short (US) region encompassing gI, gE, US9 and US2 genes and point mutations in the gC, gM, UL21 and US3 genes [110-111].

Herpesviruses as biological tools in cardiovascular research

Alphaherpesviruses are the most suitable and widely used tools for labeling neurons, but herpesviruses have yet not been used as gene delivery vectors for cardiomyocytes.

THE MAJOR AIMS OF THIS STUDY WERE AS FOLLOWS

(1) Analysis of the function of all the PRV genes under different conditions

- to characterize the kinetic patterns and compare the expression dynamics of all the 70 viral genes in the wt PRV in untreated or CHX (cycloheximede) or PAA (phosponoacetic acid)-treated PK-15 cells.
- to analyze the antisense transcription from the PRV genome

(2) Analysis of individual PRV gene functions using knockout viruses

- to analyze the effect of the *ul41* gene on the expression of the other PRV genes
- to examine the effect of individual PRV genes on the spread properties of the virus strains

(3) Development of transgenic viruses encoding

- activity sensors with which we can examine the activity of connected neurons in the brain
- differentially colored FPs and multiple colored FPs to differentiate the brain regions

Remark: In this thesis, I put a much greater emphasis on the analysis of global PRV gene expression, which is my main project, than on the utilization of PRV as a tool in biological disciplines, in which I am only a co-author.

MATERIALS AND METHODS

Cells and viruses

The entire culture procedures were performed in a class II flow hood.

Porcine kidney 15 (PK-15) cells

Monolayer cultures of immortalized PK-15 cells were used for propagation of PRV. Cells were grown in Dulbecco's Modified Eagle Medium (Sigma-Aldrich) supplemented with 5% fetal bovine serum (Gibco) and 80 μg gentamicin (Invitrogen ^{TM}) per ml, at 37 °C in an atmosphere of 95% air with 5% CO_2.

Canine cardiomyocytes

The freshly isolated cardiomyocytes were centrifuged five times at 50g for 1 minute in sterile 10% PBS (phosphate buffered saline). The supernatant was carefully removed and replaced first by 500 μM then by 1mM Ca^{2+} containing PBS solution. Most of the nonmyocytes and nonfunctional myocytes and the majority of the bacterial cells were removed by the low-speed centrifugation steps. Precipitated myocytes were resuspended in culture medium and plated on laminin precoated (1 μg/cm2) sterile coverslips at densities of up to 103 rod-shaped cells cm^{-2}. Cells were maintained 4 hours at 37°C under sterile conditions in a 5% CO_2 incubator to attach to the plate. After this time period non attached cells were removed, the plate-attached myocytes were infected with various titers of recombinant PRVs for 12 hours then washed and the culture medium was changed. Infected cells were used for analysis at various time points. After the first medium change, subsequent medium changes were carried out every day. Culture medium consisted of serum-free medium 199 (M199) supplemented with 25mM $NaHCO_3$, 5mM ceratine, 2mM L-carnitine, 5mM taurine, 100 units/ml insulin and 50 μg/ml gentamicin. (All chemicals were purchased from Sigma-Aldrich).

PRV strains

Strain Kaplan of pseudorabies virus (PRV-Ka) was used for gene expression analysis [112] and as a parental virus for producing recombinant PRVs [6, 9]. PRV strain Bartha (PRV-Ba) was also used to produce recombinant viruses [6, 113]. Experiments on gene expression were also performed using Ka-ΔVHS virus. Mutant Ka and Ba strains (Ka-ΔTK, Ba-ΔTK ΔgE/gI, ΔgE/gI/TK, and ΔTK/RR/EP0) were also used for study of individual gene functions in viral spread. Viruses were propagated in culture of immortalized PK-15 cells.

Infection conditions

The stock of the virus was prepared as follows: PK-15 cells were infected with 10 plaque forming units (pfu)/cell PRV-Ka followed by incubation of the cells until a complete cytopathic effect was observed. For the expression analysis of the PRV, rapidly-growing semi-confluent PK-15 cells were infected with a low multiplicity of infection (MOI; 0.1 pfu/cell) of the virus, and incubated for 1 h, after which the virus suspension was removed and the PK-15 cells were washed with phosphate-buffered saline (PBS). Cells were further cultivated in newly added growing medium for 0, 1, 2, 4 or 6 h. Cells were incubated in the presence or absence of 100 μg/ml cycloheximide (CHX), an inhibitor of protein synthesis, or 400 μg/ml phosphonoacetic acid (PAA), a blocker of DNA replication (both purchased from Sigma-Aldrich) 1 h prior to virus infection. Mock-infected cells, treated in the same way as infected cells, were used as controls.

We also infected PK-15 cells with high MOI (10 pfu/cell) of different PRVs: wild-type (wt) Ka, *ep0*, and *vhs*-deleted viruses. In this case, the infected cells cultivated for 0, 12, 4, 6, 8, 12, 18 or 24 hours. For the study of antisense transcription data was used from also the "high-titer" experiments of wt and *vhs*-mutant viruses. The effect of *vhs* gene on the expression of the others was tested by using the data derived from the high-titer infection. For the PRV-based delivery system the stocks of PRV were prepared by infecting PK-15 cells with of 1 pfu/cell, harvested after 24 hours, followed by freezing and thawing three times. The cells were then centrifuged and the pellet discarded. The supernatant fluid was stored in 400 μL aliquots at −80◦C.

Viral DNA preparation

Viral DNA was used for testing the primer efficiency and specificity, applied in real-time PCR. The viral DNA was isolated as follows: PK-15 cell monolayers were infected with the PRV at an MOI of 10, and cultivated at 37 °C until a complete cytopathic effect was observed. Next, culture medium was collected without disrupting the cells and clarified by centrifugation at 4,000 rpm for 10 min using a Sorvall GS-3 rotor. Subsequently, the virus in the supernatant fluids was sedimented on a 30% sucrose cushion by ultracentrifugation at 24,000 rpm for 1 h using a Sorvall AH-628 rotor. The sedimented virus was resuspended in sodium Tris-EDTA buffer. After this step, proteinase-K (l00 μg/ml final concentration) and sodium dodecyl sulfate (SDS; 0.5% final concentration) was added, and the lysate was incubated at 37 °C for 1 h. Finally, it was purified by phenol-chloroform extraction and dialysis.

Primers for reverse transcription (RT) and polymerase chain reaction (PCR)

Primers pairs were designed using the Primer Express program (Applied Biosystems) and the FastPCR Professional (Primer Digital Ltd.) oligonucleotide design software according to the given guidelines. All primers were designed to the 3'-end regions of the open reading frames (ORFs) for each gene (Table 3). The *ul26* and *ul26.5*, and *orf1* and *orf1.2* genes contain overlapping ORFs; and we therefore, did not employ distinct primers for them. Specificity of the primers was verified by BLAST searches of the GenBank database (National Center for Biotechnology Information (NCBI) website (http://www.ncbi.nlm.nih.gov/BLAST/). Oligonucleotide primers were purchased from Bio Basic Inc. (Mississauga, Ontario, Canada).

Polymerase chain reaction (PCR)

A traditional, end-point PCR technique was used to check the potential genomial DNA contamination. Primer specificity and quality also was tested by running PCR reactions by using the GC Rich PCR System in accordance with the manufacturer's instructions (Roche Diagnostics GmbH) and a Veriti™ 96-Well Thermal Cycler (Applied Biosystems) according to the protocol: 1 cycle of 4 min at 94 °C; 30 cycles of 1 min at 94 °C, 60 °C for 1 min and 72 °C for 2 min; and 1 cycle of 72 °C for 7 min.

The complete PRV genome sequence is a composite of 6 different strains (Becker, Indiana-Funkhauser, Ka, NIA-3, Rice, and TNL) [10], the percentage of nucleotide identity between them is approximately 99%. Most of the sequence data (86.7%) have been derived from strain Kaplan (PRV-Ka), which were used in our experiments. To circumvent the problem of genetic background differences, we tested 2 or more primers for RT and PCR reactions for non-Ka sequences and selected those that performed best; alternatively, we sequenced the particular DNA region and designed new primers based on the sequence data. For all genes, we tested several primers to optimize the reactions and selected those, which did not produce primer dimers or other nonspecific products. To minimize the primer dimmer effects in case of that genes where we could not eliminate them, a detection step ("extra extension step") was applied in every cycle after the extension with a temperature approximately 3°C below the melting temperature (Tm) of the specific PCR product, but well above the Tm of the primer dimers) for the detection.

RNA preparation

PK-15 cells ($5x10^6$ cells per flask) were washed in PBS and harvested for RNA purification at 0, 1, 2, 4 and 6 h pi. Total RNA was isolated from the cells with the NucleoSpin RNA II Kit (Macherey-Nagel GmbH and Co. KG) as recommended by the manufacturer. Briefly, cells were collected by low-speed centrifugation, lysed in a buffer containing the chaotropic salts, which inactivates RNases and allow nucleic acids to bind to silica membranes.

Samples were treated with RNase-free rDNase solution (included in the Kit) to remove potential genomic DNA contamination. Subsequently, the possible residual DNA contamination was removed by using Turbo DNase (Ambion Inc.). As a final step, RNA samples were eluted in RNase-Free Water (supplied with the Kit) in a total volume of 60 µl. The measurement of RNA concentrations were quantified in triplicate by spectrophotometrically by measuring the absorbance at 260 nm in a BioPhotometer Plus (Eppendorf). The RNA solution was stored at -80 °C until use.

Quantitative real-time RT-PCR

A reverse transcriptase based quantitative real-time PCR was carried out for the transcriptional analysis. For each gene, a minimum of 3 parallel independent samples (separate infections) were used.

Reverse transcription (RT)

Total RNA extracted from infected cell cultures subjected to drug treatment (CHX or PAA) was transcribed into cDNA for real-time PCR analysis. RT reactions were performed in a total volume of 5 μl of solution containing 0.07 μg of total RNA, 0.25 μl of dNTP mix (10 μM final concentration), 2 pmol of the gene- and strand-specific primer, 1 μl of 5x First-Strand Buffer, 0.25 μl (50 units/μl) of SuperScript III Reverse Transcriptase (Invitrogen) and 1U of RNAsin (Applied Biosystems Inc.). RT mixtures were incubated at 55 °C for 60 min. The reaction was stopped by raising the temperature to 70 °C for 15 min. No-RT control reactions (RTs without the reverse transcriptase enzyme) were run to test the potential viral DNA contamination by conventional PCR. RNA samples with no detectable DNA contamination were used for quantitative RT-PCR reactions. First-strand cDNAs were diluted 10-fold with Gibco UltraPure DEPC-treated, RNase- and DNase-free distilled water (Gibco/Invitrogen), and then subjected to real-time PCR analysis.

Real-time PCR

Real-Time PCR experiments were performed by using the Rotor-Gene 6000 thermal cycler (Corbett Life Science). All reactions were carried out in 20-μl reaction mixtures containing 7 μl of cDNAs, 10 μl of ABsolute QPCR SYBR Green Mix (Thermo Fisher Scientific), 1.5 μl of forward and 1.5 μl of reverse primers (10 μM each). The running conditions were as follows: (1) 15 min at 95 °C, followed by 30 cycles of 94 °C for 25 sec (denaturation), 60 °C for 25 s (annealing), and 72 °C for 6 s (extension). The absence of nonspecific products or primer dimers was indicated by observation of a single melting peak in melting curve analysis. An additional extension and detection step was applied for those primers that produced primer dimmers: for 2 s at a temperature just below the Tm of the specific product and substantially above the Tm of the primer dimers. With this technique we could eliminate nonspecific fluorescent signals produced by primer dimers. Following the PCR reaction, melting curve analysis was performed to control amplification specificity (specificity was defined as the production of a single peak at the predicted temperature and the absence of primer dimers) by measuring the fluorescence intensity across the temperature interval from 55 °C to 95 °C. The 28S ribosomal (r)RNA used as the loading control (reference gene) was amplified in each run. H_2O was included as a no-template control, and cDNA derived from the reverse-transcribed RNAs of non-infected cells was used as a negative mock-infected control. We applied SYBR Green-based real-time PCR because of the lower costs and simpler protocol than for TaqMan probe-based methods for instance. It has recently been demonstrated that the SYBR-based method of detection is as sensitive and specific, and has a similar dynamic range to that of the TaqMan-based technique [114].

Statistics

Calculation of relative expression ratio (R)

We calculated the R value by using the following mathematical model:

$$R = \frac{(E_{sample\max})^{Ct_{sample\max}}}{(E_{sample})^{Ct_{sample}}} : \frac{(E_{ref\max})^{Ct_{ref\max}}}{(E_{ref})^{Ct_{ref}}} \quad ,$$

where R is the relative expression (quantification) ratio or relative copy number; E is the amplification efficiency of one reaction cycle; Ct is the threshold cycle value; sample refers to any particular gene at a given time point; and ref is the 28S rRNA, which was used as a reference gene and was amplified in each run. Average Ct values with their standard error (SE) values and amplification efficiencies with SE are shown in the reference [112]. This equation is a modification of the "Soong's formula" [115], using the average maximal value

of E^{Ct} for each gene as the control instead of individual values. The relative expression ratios of mRNAs were calculated by normalizing cDNAs to 28S rRNA using the Comparative Quantitation module of the Rotor-Gene 6000 software (Version 1.7.28, Corbett Research), which automatically calculates the real-time PCR efficiency sample-by-sample. Thresholds were set automatically by the software.

Calculation of the modified R values: R_a, R_Δ, $R_{i\text{-}PAA}$ and $R_{i\text{-}CHX}$

R_a: rates of change was calculated using the following formula: $R_a=R_{(t+1)}/R_t$

R_Δ: the net increase between two time points was calculated as follows: $R_\Delta=R_{(t+1)}-R_t$

$R_{i\text{-}PAA}$: the inhibitory effect of PAA on gene expression was calculated by using the ratio of the R values for the PAA-treated/untreated samples at each individual time points.

$R_{i\text{-}CHX}$: the inhibitory effect of CHX on gene expression was calculated by using the ratio of the R values for the CHX-treated/untreated samples at each individual time points.

Analysis and presentation of Real-Time PCR data

Data were analyzed by the Microsoft Excel program, using the average and the standard deviance functions. The inhibitory effect of CHX or PAA was calculated via the ratio of the drug-treated and untreated R values at 2, 4 and 6 h pi for CHX: $R_{i\text{-}CHX}=R_{CHX}/R_{UT}$, or 4 and 6 h pi for PAA: $R_{i\text{-}PAA}=R_{PAA}/R_{UT}$. Thus, a low value indicates a high inhibitory effect and *vice versa*. The net increase in a product was calculated by subtracting the R value at time point t+1 from that at t ($R_\Delta=R_{(t+1)}-R_t$), where t = 0, 1, 2, 4 or 6 h and (t+1) = 1, 2, 4 or 6 h. The ratios of adjacent R values (rate of change; R_a) were calculated with the following equation: $R_a=R_{(t+1)}/R_t$; t = 1, 2, 4 or 6 h; (t+1) = 2, 4 or 6 h. Pearson's correlation analysis was used to evaluate qRT2-PCR data, as an alternative method for the grouping of PRV genes into kinetic classes. Pearson's correlation coefficient (r) was calculated as follows:

$$r=\frac{\sum_{i=1}^{n}(X_i-\overline{X})(Y_i-\overline{Y})}{(n-1)S_xS_y}$$

A correlation is a number between -1 and +1 that measures the degree of association between two variables [labeled here as X and Y, which are the R_Δ values of two different genes in the same time interval (i)]. $\overline{X}$ and $\overline{Y}$ are the average values, n is the sample number, and S_X and S_Y are the standard deviances (errors) for X and Y, respectively. A positive value for the correlation implies a positive association and a negative value implies a negative or inverse

association. Genes were clustered by using a complete linkage hierarchical clustering method with a centered correlation similarity metric with Cluster 3.0 program (Stanford University). To view the clustering results generated by Cluster 3.0, we used Alok Saldanha's Java TreeView software.

Gel electrophoresis

Larger DNA fragments generated by using conventional PCR cycler were run on 1% agarose/TBE gels containing ethidium bromide (EtBr) and visualized under UV illumination, using Marker 16 (Lambda DNA/*Eco*130I; Fermentas) to size DNA fragments. Smaller DNA fragments generated by qRT2-PCR were run in a 12% polyacrylamide gel to determine if the amplified products are of the correct size. To visualize the DNA fragments, the EtBr-stained gels were placed on UV transilluminator. A GeneRuler™ Low Range DNA Ladder (Fermentas) was included in each run.

Restriction endonuclease (RE) analysis

To make sure the amplified RT^2-PCR products are specific, RE analysis was performed.

Construction of recombinant plasmids

Plasmids containing PRV DNA fragments were constructed for DNA sequencing analysis, which was performed when the specificity of amplicons generated by real-time PCR was uncertain; or if primers designed on the basis of sequence data relating to non-Ka strains performed badly. PRV DNAs were subcloned by using two methods: PCR amplification of the particular DNA segment; or subcloning of the desired DNA region by standard molecular cloning protocols. Amplified products were subcloned to the pGEM (Promega) vector following the manufacturer's descriptions. PRV *Bam*HI fragments to be sequenced were subcloned to the pRL525 vector [116].

DNA sequencing

Subcloned DNA fragments were subjected to DNA sequencing with the ABI Prism™ 3730xl DNA sequencer (AME Bioscience Ltd.). DNA sequences were analyzed by using the Chromas Lite 2.01 software (Technelysium Pty Ltd).

Construction of targeting vectors

Targeting vectors were used to deliver reporter genes and/or mutations to the PRV genome. A typical targeting plasmid was constructed by the insertion of a marker gene expression cassette to an internal position of a previously subcloned viral DNA segment, which provided homologous flanking sequences for recombination with the desired integration site in the PRV genome.

Flanking sequences

PRV DNA segments of interest were subcloned into members of a palindrome-containing positive-selection vector family (pRL479, pRL525) or pBlueScript II KS plasmid. Subsequently, viral DNA sequences were cut with one or two unique restriction endonucleases (REs), followed by Klenow filling-in of 5'f-overhangs (in case of sticky ends) and insertion of either an *Eco*RI or a *Hind*III linker, which served as a cloning site for the incorporation of reporter gene expression cassettes [6].

Reporter genes

Several reporter genes were fused with MARCKS[2] (myristoylated alanine-rich C-kinase substrate) to create membrane targeted fluorescent proteins (e.g. memOrange, memTFP). Expression cassettes were modified to contain either *Hind*III or *Eco*RI RE sites at both ends for subcloning into flanking viral sequences. We also engineered multiple color expressing viruses which express different fluorescent proteins (e. g. orange, teal, red) [6].

Modification of the gE and gI coding region

The first step in the generation of gE/gI deletion-based flanking sequence was to the *Bam*HI-7 fragment of the PRV genome - containing the gE and gI coding region - was isolated and subcloned to pRL525 cloning vector. Its 1855-bp *Stu*I – *Age*I DNA fragment was replaced by an *Eco*RI linker. The removed *Stu*I – *Age*I fragment resulted in the inactivation of both gE and gI genes of the virus. Reporter genes were ligated to the *Eco*RI site of the construct.

Neut region

The DsRed2 (Clontech Laboratories Inc.) is an engineered monomeric red fluorescent protein (RFP) from *Discosoma sp*. The *Bam*HI8' fragment, which contain the Neut region of the virus genome was subcloned into the pRL525 plasmid. *Stu*I unique restrictrion site (located in the Neut region) was replaced by *Eco*RI linker. The DsRed was ligated to the *Eco*RI site of the plasmid.

Construction of the TK-expression cassette

TK gene of HSV was inserted into the pUCB vector. The gene was controlled by transcription regulatory sequences (pCMV and SV40 PolyA).

Generation of PRV amplicon constructs

We have generated modified virus vectors (amplicons): amplicon-memCherry (amp-memCherry), amplicon-memCerulean (amp-memCerulean) and amplicon-memGFP (amp-memGFP). The *OriS* and *PAC* regions of the PRV genome were amplified by PCR than subcloned into pBlueScript II KS plasmid. Several FPs (membrane bound red, blue and green fluorescent proteins: memCherry, memCerulean and memGFP respectively) were also inserted to the *Eco*RI recognition site of the plasmid. Reporter genes were driven by the human cytomegalovirus immediate early 1 promoter (pCMV) and terminated by the simian virus SV40 polyadenylation sequence.

Creation of ep0 gene targeting vector

The *Kpn*I-F DNA fragment containing the sequence of the *ep0* gene was cloned into the pRL525. Next, it was cleaved with *Bam*HI RE to remove the 1388 bp *Bam*HI fragment including the entire *ep0* gene. Subsequently, free DNA ends were filled up by Klenow enzyme followed an *Eco*RI linker insertion. The lacZ gene expression cassette was subcloned to the *Eco*RI site of this plasmid.

Generation of the RR gene targeting vector

Firstly, a 5-kbp *Sal*I-F fragment of the virus DNA containing both subunits of RR (large: RR1 and small: RR2) gene was isolated and subcloned into the pRL494, [34], which was cut with *Sca*I and *Mlu*I REs generating a 1805-bp deletion. This deletion included a 1789-bp DNA sequence from the 3' of RR1 and a 7-bp DNA sequence from the 5' end of RR2 of ribonucleotide reductase gene. As a next step, free DNA ends were converted to *Eco*RI sites via Klenow filling and attaching *Eco*RI linker to the blunt DNA ends. Finally, a lacZ gene expression cassette flanked by *Eco*RI sites was subcloned to the *Eco*RI site of this plasmid.

ASP (putative antisense promoter) region

The *Bam*HI-8'-F PRV DNA fragment (4.9 kb) was isolated and subcloned to pRL525 cloning vector. The *Dra*I site of the putative TATAA box of ASP sequence was converted to *Eco*RI by linker insertion destroying its function and generating pASP-RI. Alternatively, *Bam*HI-8'-F fragment was subcloned into pRL479 followed by conversion of the *Dra*I site to *Hind*III resulting in pASP-HIII. As a final step, the various reporter gene expression

cassettes were inserted either into the *Eco*RI site of pASP-RI (GFP, lacZ, troponeon), or the others into the *Hind*III site of pASP-HIII, resulting in the generation of ASP-based targeting constructs.

Transfection

Fluorescent protein-encoding plasmids were transfected to PK-15 cells with Lipofectamine™ transfection reagent (Invitrogen ™) following the manufacturer's recommendations.

Generation and isolation of recombinant viruses

Recombinant viruses were generated by means of homologous recombination between parental virus genomes and the homologous sequences of the targeting plasmids (Table 1. shows the recombinant viruses constructed by me). Actively growing PK-15 cells were co-transfected with viral DNA and the linearized targeting vector with lipofectamine-mediated gene delivery (Lipofectamine 2000 Reagent, Invitrogen). Plaques formed by FP-carrying recombinant viruses were screened based on their fluorescence or the lacZ gene-expressing PRVs were detected by blue plaque assay using 5-bromo-4-chloro-3-indolyl-*b*-D-galactopyranoside (XGal), the chromogenic substrate of *β*-galactosidase. Recombinant viruses were isolated by 6-15 cycles of plaque purifications using a fluorescence microscope (Olympus IX-71). Deletions in the viral genome without reporter gene insertion were generated by insertion and subsequently elimination (via empty flanking sequences) of the FP or lacZ expression cassette.

Activity sensor PRVs

Gene encoding, fluorescence resonance energy transfer (FRET)-based fluorescent Ca^{2+} indicators (TN-L15, troponeon [117] were inserted to the PRV genome (either to the Ka, or to the Bartha strain). Troponeon expressing PRVs were under the control of the major immediate early promoter of human cytomegalovirus (CMV promoter) developed activity sensor PRVs that report the activity of the infected cells. The marker gene expression cassette also contained simian virus 40 (SV40)-derived sequences (eg. polyA (polyadenylation) signal and transcription termination sequences). Additionally, a lacZ gene was also used as a reporter gene for the identification of mutant viruses.

Name	Genome	Mutation location	FP/Marker gene
memTeal-PRV	Ka	gE/gI	memTFP
mem-Orange-PRV	Ka	gE/gI	memOrange
Red-PRV	Ba	Asp	DsRed2
Ba-DsRed	Ba	Neut	DsRed
Ka-RR/ep0/Asp/Tropo	Ka	RR/ep0/Asp	Troponeon
ΔTK	Ba	TK	- (Colorless)
ΔVHS	Ka	VHS	LacZ

***Table 1**. **Recombinant PRV strains** with their colors and the locations of their mutations.*

Generation of Ka-VHS-Lac virus strain

The 2526-bp *Xho*I DNA fragment containing the entire VHS gene was subcloned to the pRL494 vector *Sal*I site. The unique *Nru*I site of this DNA segment was replaced by an *Eco*RI site by linker insertion, which resulted in a frameshift mutation in the VHS gene. A lacZ expression cassette was used as a reporter gene, controlled by CMV promoter (pCMV). This construct was co-transfected with Ka PRV, and Ka-VHS-Lac virus was made by homologous recombination.

Generation of ΔTK viruses

The *Bam*HI11 fragment (containing the TK gene) of the virus genome was subcloned to the pRL425 vector. This construct was double-digested (cut) with *Nru*I and *Xho*I REs. The *Xho*I site was filled in with Klenow than a *Hind*III linker was inserted. The *Hind*III was converted to *Eco*RI linker (which served as a cloning site). It was cut with *Bam*HI and inserted into a pRL494 (digested with *Bgl*II; resulting in pRL494-TK6Δ*Eco*RI). Monomeric (m) and membrane-bound (mem) fluorescent protein (memCerulean, memCherry, mGFP, mRFP) expressing cassettes (FPs driven by pCMV, terminated by SV40 PolyA and ligated to *Eco*RI linkers) were inserted into the *Eco*RI site of the plasmid. This construct was co-transfected with Ba or Ka PRV DNA resulting in the introduction of FP genes to the virus DNA by homologous recombination.

Construction of colorless KO viruses

Following the introduction of the FP gene into the genome of the ΔTK-PRV, a new co-transfection experiment has been carried out with the FP-encoding ΔTK virus DNA and the pRL494-TK6Δ*Eco*RI. Colorless recombinant viruses were selected on the basis of their non fluorescent phenotype.

RESULTS

Whole-genome analysis of wild-type (wt) PRV

Kinetic classes of PRV genes on the basis of dependence of gene expression on DNA replication and de novo protein synthesis

To test the dependence of the PRV genes on DNA synthesis, we treated the PRV-infected PK-15 cells with PAA, a blocker of DNA replication. Figure 3 shows the order of the PRV genes ranked on the basis of 6h $R_{i\text{-}PAA}$ values [112].

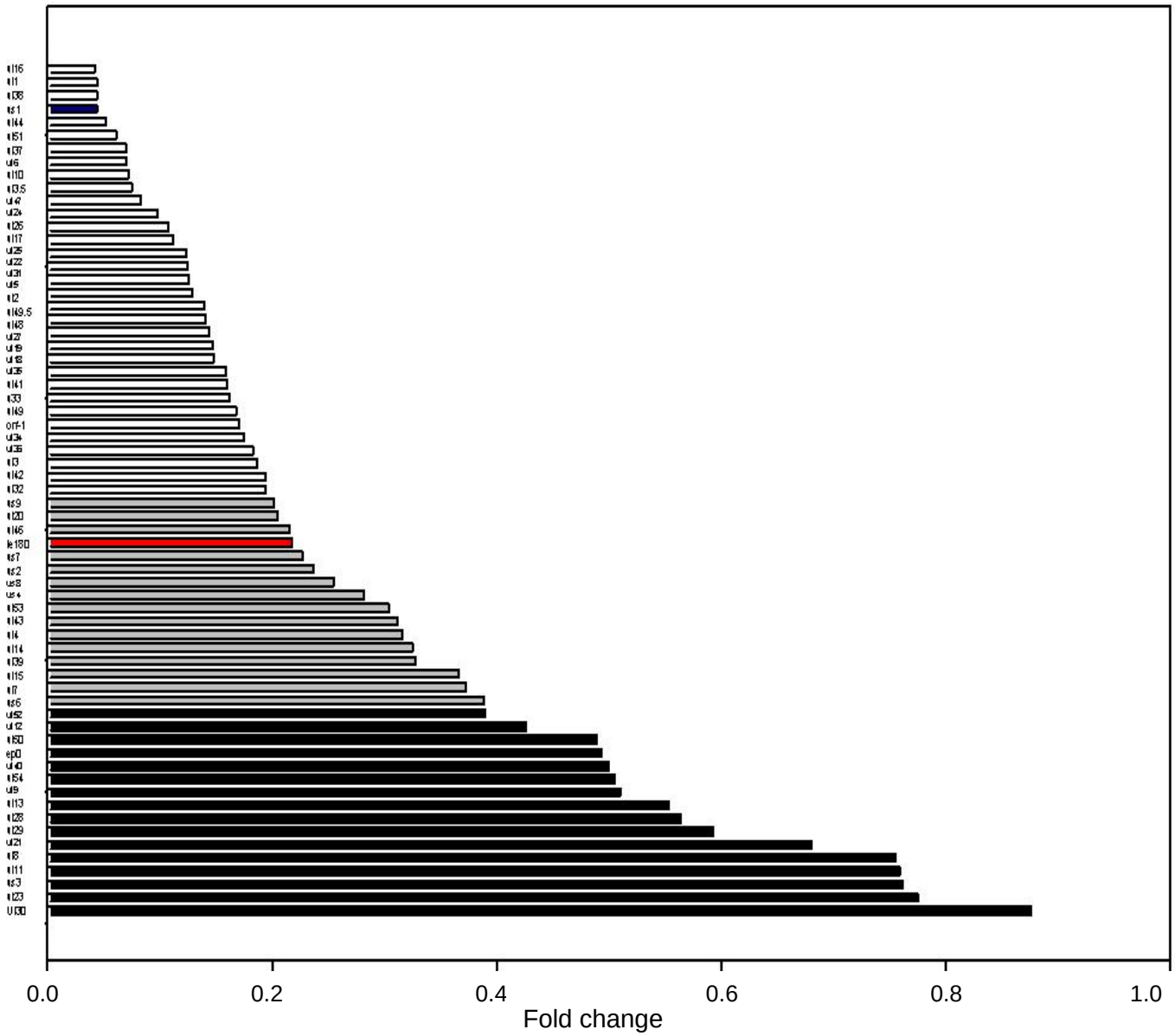

Figure 3. *PRV genes ranked on the basis of 6h $R_{i\text{-}PAA}$ values. White bars indicate late genes, grays are the early-late, black bars represent the early genes, blue and red represents the two regulatory genes, the us1 and the ie180, respectively.*

Our result shows that PAA exerts a drastic effect on the expression of L genes (these genes have the lowest $R_{i\text{-}PAA}$ values), while it inhibits E gene expression to a lower extent (they have higher $R_{i\text{-}PAA}$ values). This phenomenon is explained by the fact that the gene expression is dependent on the promoter activity as well as on the copy numbers of genes which are higher after the viral genome replication than at the initial stage of infection when the PRV DNA is represented in a single copy per cell in our system). As figure 3 shows, it is not possible to draw a sharp line between the E and L genes; there is rather continuity between the kinetic classes. All protein-coding PRV genes have been well categorized by PAA analysis, except the *ie180* gene which displays a unique expression pattern. We compared our results with the previously published kinetic groups of HSV and PRV genes. It is known that there is a certain degree of disagreement between the authors in the categorization of HSV genes. Furthermore, a complete expression data set for the PRV genes is not available [112].

Table 2 shows the PRV genes and their kinetic classes based on our PAA experiments, and also the categories established by earlier studies (collected by Mettenleiter), as well as the kinetic properties of the homologous genes of HSV (based on the studies conducted by Wagner and Roizmann's groups). We also tested the effect of the absence of *de novo* protein synthesis on PRV gene expression. As Figure 4 shows, the IE180 product displayed a significantly increased level of expression in the CHX-treated samples in each analyzed time points: 2.27-fold at 2 h; 5.55-fold at 4 h; 1.4-fold at 6 h pi.

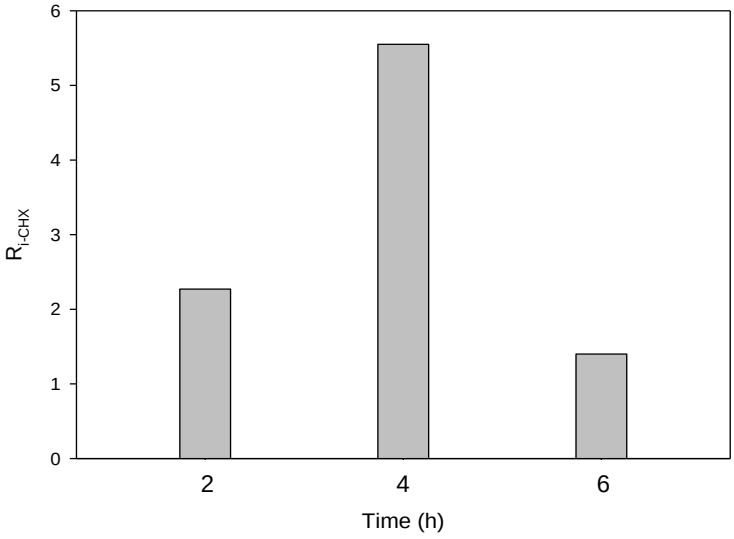

Figure 4. *The effect of CHX on the expression of ie180 at 2, 4 and 6 h pi.*

The CHX-mediated inhibition of viral gene expression ($R_{i\text{-}CHX}$) was calculated as follows: $R_{i\text{-}CHX} = R_{CHX}/R_{UT.}$

The explanation of this phenomenon is that the IE180 protein binds to its own promoter and thus, inhibits its own synthesis [122], but in the case of the CHX-treated samples, no negative feedback is exerted by IE180 due to the lack of this DNA-binding protein. The inhibitory effect of CHX on the transcription of the other protein coding PRV genes is very strong: the

degree of inhibition [1-$R_{i\text{-}CHX}$) × 100] was found to range between 97.3 and 100%. Our CHX analysis revealed that PRV has only one true IE protein-encoding gene, which is the *ie180*.

Name	**Transcription Kinetics**							**Function**	**References**
	Wagner[37]	**Wagner[38]**	**Roizman[39]**	**Roizman[40]**	**Mettenleiter[41]**	**Mettenleiter[41]**	**Our data**		
orf-1							L	unknown	
*ul54 (*ICP27)*	IE	IE	IE	IE	IE	E	E	*transcription regulation*	123
ul53 (gK)	L	EL	L	L	L	(EL) 3h pi	E/L	viral egress	123
ul52	E	E	E	E	E	(E) 2h pi	E	*DNA replication*	123
ul51	L	EL	L	L	L	E	L	viral egress/oralgen unknown	123
*ul50 (*dUTPase)*	E	E	E	E	E	(EL) 3h pi	E	dUTPase, viral replication	30
ul49.5 (gN)	L	L	L2	L2	L	L	L	virion entry	124
*ul49 (*VP22)*	E?	E	L	L	E	(EL) 4h pi	L	virion formation, tegumentation	30
*ul48 (*VP16, α-TIF)*	?	EL	L	L	L	(L) 8h pi	L	gene regulation, viral egress	125
*ul47 (*VP13/14)*	E	EL	L2	L2	L	L	L	secondary envelopment	125
*ul46 (*VP11/12)*	E	EL	L	L	L	E	E/L	unknown function, tegument protein	125
ul27 (gB)	E	EL	L1	L1	E	ND	L	cell-cell spread, virus entry	30
*ul28 (*ICP18.5)*	E	EL	L	L	E	E	E	DNA cleavage and packaging	30
*ul29 (*ICP8)*	E	E	E	E	ND	ND	E	DNA replication	30
ul30	E	E	E	L	E	ND	E	*DNA replication*	30
ul31	L	EL	L2	L2	L	(L) 6h pi	L	nuclear egress	126
ul32	L	EL	L2	L2	L	ND	L	*DNA packaging*	3
ul33	L	EL	?	L	L	ND	L	*encapsidation of viral DNA*	127
ul34	L	L	?	L	ND	(EL) 3h pi	L	nuclear egress	15
*ul35 (*VP26)*	L	L	L2	L2	L	ND	L	*capsid protein*	128
*ul36 (*VP1/2)*	?	EL	L2	L2	L	(EL) 3-9h pi	L	tegumentation and egress	70
ul37	L	E	L	L	L	(E) 2h pi	L	secondary envelopement, egress	70
*ul38 (*VP19c*)	L	L	L2	L2	L	(E) 2h pi	L	**capsid protein*	129
ul39 (RR1)	E	E	E	E	E	(E) E/L	E/L	nucleotide synthesis	129
ul40 (RR2)	E	E	E	E	E	E	E	nucleotide synthesis	130
ul41 (VHS)	L	EL	L	L	L	ND	L	*RNase, gene regulation*	131
ul42	L	E	E	E	E	L	L	DNA replication	130
ul43	L	EL	?	L	E	E	E/L	unknown	132
ul44 (gC)	L	L	L2	L2	L	L	L	viral entry, virion attachment	133
ul26	E	L	L	L	L	L	L	scaffold protease	135
ul25	L	EL	L	L	L	L	L	capsid protein	134
*ul24 (*VP24)*	L	L	L	L	L	L	L	*unknown*	135
ul23 (TK)	E	E	E	E	E	E	E	nucleotide synthesis	130
ul22 (gH)	L	L	L2	L2	L	L	L	viral entry, cell-cell spread	130
ul21	L	E	?	L	L	L	E	capsid maturation	130
ul20	L	EL	L	L	L	ND	E/L	capsid transport	3
*ul19 (*VP5)*	L	EL	L1	L1	L	(L) 16h pi	L	*capsid protein*	136
*ul18 (*VP23)*	L	EL	L	L	L	ND	L	*capsid protein*	30
ul17	L	EL	L	L	L	ND	L	*DNA cleavage and encapsidation*	3
ul16	?	EL	?	L	L	ND	L	*unknown, interacts with UL11*	30
ul15	L	EL	L	L	L	ND	E/L	*DNA cleavage and encapsidation*	30
ul14	L	EL	?	L	L	L	E/L	*DNA cleavage and packaging*	130
*ul13 (*VP18.8)*	L	EL	L	L	L	(E) EL	E	protein phosphorylation	130
*ul12 (*AN)*	E	E	E	E	E	(E) EL	E	alkaline nuclease	130
ul11	L	EL	L(?)	L	L	L	E	secondary envelopement	130
ul10 (gM)	L	E	L	L	L	E	L	egress, secondary envelopement	137
*ul9 (*OBP)*	E	E	L(?)	E	E	E	E	**ori depentent DNA synthesis*	137
*ul8 (*OBPC)*	E	E	E	E	E	(E/L) 3-5h pi	E	*DNA replication*	137
ul7	?E	E	?		L	(E/L) dE	E/L	unknown	137
ul6	L	E	?		L	(E/L) dE	L	*capsid protein, portal protein*	137
ul5	E	E	E	E	E	(L) 6h pi	L	*DNA replication*	138
ul4	E	E	?	L	L	(L) 6h pi	E/L	*unknown*	138
ul3.5						E/L	L	replication, cell-to-cell spread	138
ul3	L	L	L2	L2	L	E/L	L	unknown	138
*ul2 (*UNG)*	E	E	E	L	E	E/L	L	*DNA repair*	138
ul1 (gL)	E	EL1	L	L	L	E/L	L	viral entry, cell-to-cell spread	138
*ep0 (*ICP0)*	IE	IE	IE	IE	E	E	E	gene regulation	10
*ie180 (*ICP4)*	IE	IE	IE	IE	IE	IE	E/L	gene regulation	13
*us1 (*RSp40/ICP22)*	IE	IE	IE	IE	IE	IE	L	*regulator of gene expression* .	30
us3(PK)	E	E	E	E/L	E	E	E	nuclear egress	30
us4(gG)	E	E	L	L	E/L	E	E/L	unknown	139
us6 (gD)	L	E	L1	E/L	E/L	ND	E/L	entry	30
us7 (gI)	E	E	L	L	L	(L) 6h pi	E/L	cell-to-cell spread	30
us8 (gE)	E	E	L2	L2	L	E	E/L	cell-to-cell spread	140
*us9 (*11K)*	E	E	?	L	L	L	E/L	anterograde spreed of virus	141
*us2 (*28K)*	E	E	?	L	L	(L) 5h pi	E/L	*unknown*	30

Table 2. *Function and kinetic classification of PRV genes*

Characterization of the kinetic properties of the PRV genes in untreated cells

Traditionally, herpesvirus genes are classified on the basis of the effects of transcription and translation inhibition on their expression. The high- throughput and very sensitive Real-time RT-PCR technique allows the analysis of the expression dynamics of PRV genes and the classification of viral mRNAs without drug treatment. PRV genes were ranked on the basis of their relative expression ratios (Rs) at different time points. At 1 and 2 hours post-infection (pi) typical E genes are at the top of the list (E genes have the highest R values at the early stage of infection), while L genes at the end of the list. At 1h and 2 h pi the *ul30* gene has the highest R (R_{1h} and R_{2h}) value among the protein-encoding genes and intriguingly, this product has the highest net increase within the interval 1-2 h pi. This transcript is the highly abundant, as indicated by the low Ct values at each time period. These results indicate that the majority of DNA polymerase mRNAs are already produced in the early phase of PRV infection.

The IE180 transcripts are the only mRNAs whose amounts significantly decline (by 27.6%) between 1 and 2 h. R_{4h} values show that the E genes are close to their maximal values by 4 hour pi, but the L genes are still far from their peaks. Each protein coding gene riches its highest R value at 6h pi, except *us3*, which has its maximal R value at 4h pi. A characteristic feature of L gene transcripts is that their R_{Δ} values (net increase between two time points) are low between 0-1 h and high between 4-6 h. Our data show that the R_a of L gene transcripts are higher than R_a of E genes in the 2-4 h infection period, which is explained by the low R values of the L genes at 2 h pi. Between 4-6 h time points, both the R_{Δ} and R_a of the L gene mRNAs are higher than those of the E genes. Comparison of the ranking of the genes on the basis of their $R_{6\ h}–R_{4\ h}/R_{1\ h}$ and $R_{i\text{-}PAA}$ values shows a significant similarity, which means that viral genes can be classified by analyzing the gene expression without drug treatment [112].

Define the expression pattern of the whole PRV genome

Based on the R_{Δ} values, using the Pearson's correlation coefficients (r), we clustered the PRV genes into 10 different groups. This coefficient expresses the kinetic properties of a gene pair in a single number. Genes were grouped to the same cluster, when their pairwise r values exceeded 0.9. R_{Δ} values were also used to group the genes by the hierarchical clustering method. Figure 5 shows a heatmap combined with a dendogram based on the hierarchical clusterization. Figure 6 shows the running curves of a typical E gene and a typical L gene and 3 genes with unique expression profiles according to the Pearson's correlation coefficients [112].

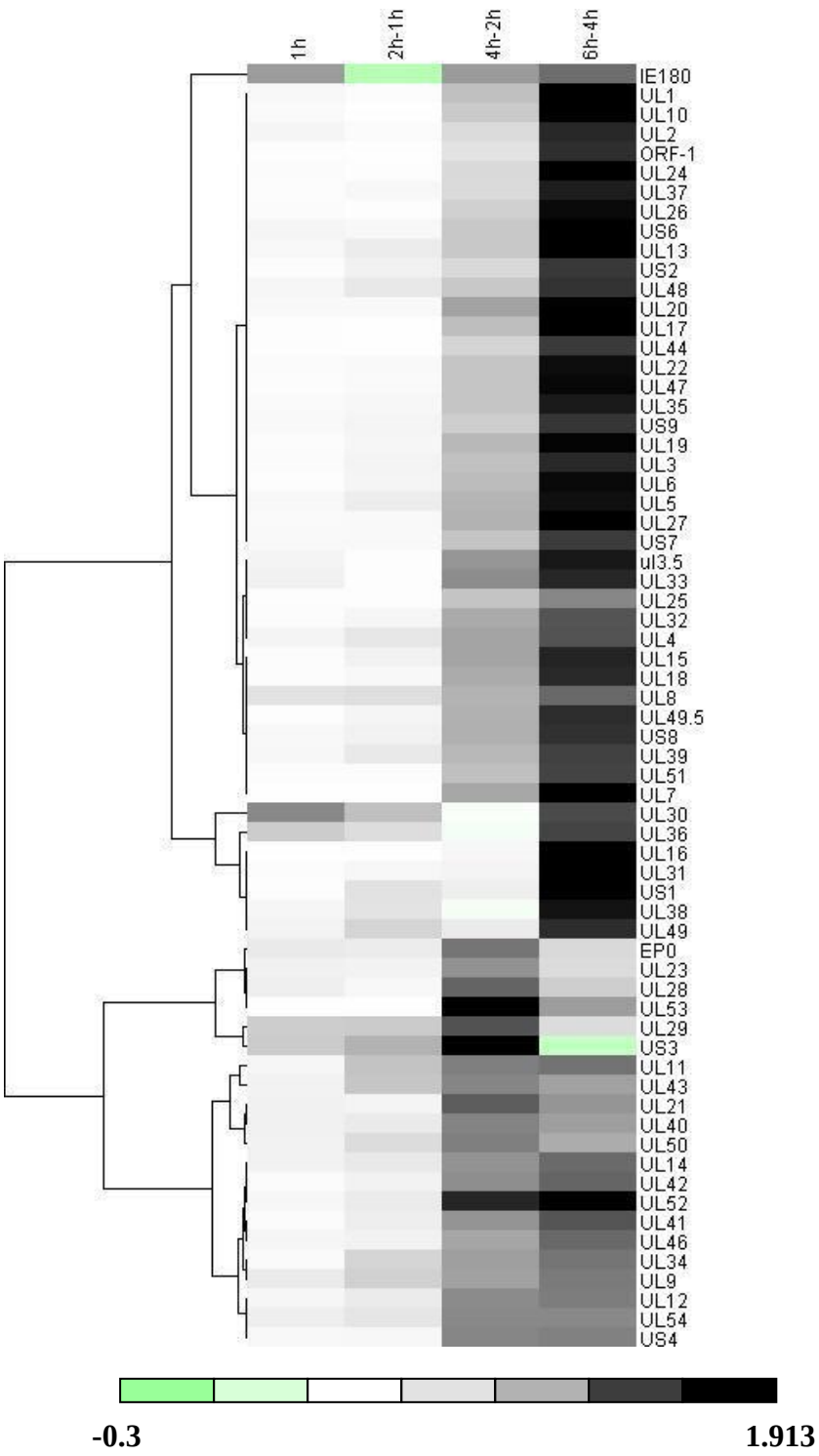

Scale of R_{Δ} values

Figure 5. *Heatmap with dendogram of PRV gene clustered on the basis of their R_{Δ} values. The heatmap depicts the whole-genome profiling of protein-coding PRV genes, following de novo infection of PK-15 cells. Green color indicates negative R_{Δ} values, white color are low positive, while grey color are positive intermediate R_{Δ} values, and black indicates the highest level of increase in viral mRNA detected between two time points.*

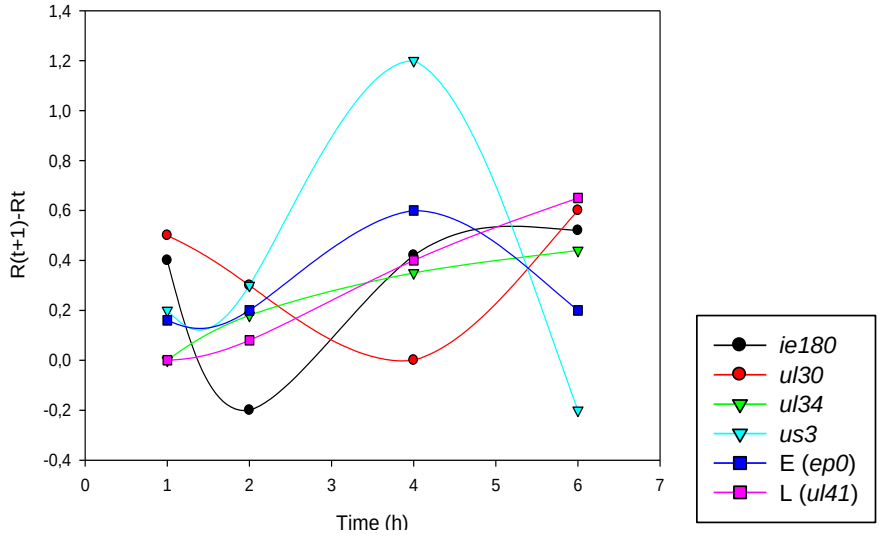

Figure 6. The expression curves of 6 genes. *Pearson's correlation analysis was performed for clustering of PRV genes into groups on the basis of their similar expression dynamics (using pairwise R_{Δ} values) across the examination period. The early genes have the highest net increase between 2 and 4 h pi, while they decrease after 4h pi. The ep0 represents the E genes. The late genes rich their highest R values at 6 h pi. The plot of ul41 shows the typical expression dynamics of L genes. The ie180, ul30, ul34 and us3 show unique expression profiles.*

Detection and analysis of antisense RNAs

Using strand-specific primers for the reverse transcription, it was possible to detect transcription from both DNA strands. Due to the sensitivity of the Real-time RT-PCR technique, we detected antisense transcription from the opposite strand of almost every protein coding gene both in high and low MOI infection. The figures 7 A and B show the expression dynamics of two antisense transcripts [the long-latency transcript-1 (*LLT1*), and the long-latency transcript-2 (*LLT2*)], as well as and their sense partners (EP0 and IE180 mRNAs). *Llt1* and *llt2* are antiparallel to *ep0* and *ie180*, respectively. LLTs of PRV are the only transcript made during latent viral infection [112].

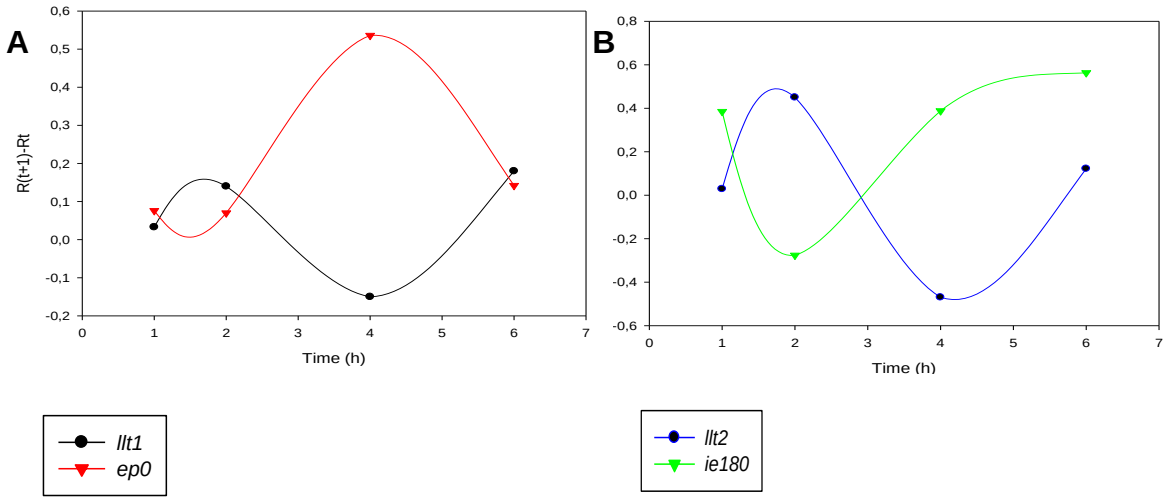

Figure 7. Expression curves of the LLTs and their mRNA partners. A.*The ep0 and its antisense partner (llt1) show inverse expression profile.* ***B.*** *The expression curves of R_{Δ} reveal show an inverse relationship between the ie180 mRNAs and its antisense transcript, llt2.*

Figure 8 shows the $R_{i\text{-}CHX}$ values of the LLTs. The transcript of the *llt2* significantly increase (except at 6 h pi), while the *llt1* is blocked by CHX. These results suggest that the LLT2 is an IE transcript and that the IE180 protein exerts negative effect on its expression.

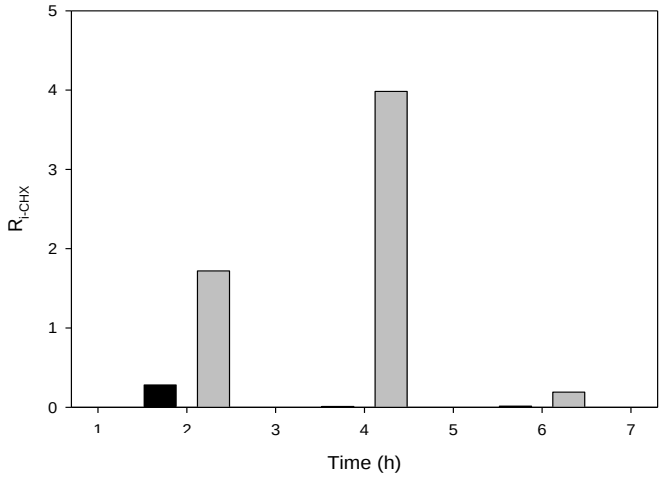

Figure 8. The inhibitory effect of CHX on the LLTs *at 2, 4 and 6 h pi. The expression of the llt1 is blocked by the CHX, while, as in IE180 mRNA, the expression level of its antisense partner is increased at 2 and 4 h.*

Figure 9 shows the effect of PAA on the expression of LLTs. The LLT displays an unusual response to PAA treatment. Namely, the level of LLT1 increases to 2.94-fold at 4h, and drops at 6h pi (to 0.007-fold) relative to the untreated sample; while the level of LLT2 increases markedly (close to 40-fold at 4 h, and 3-fold at 6 h pi) (this phenomenon will be discussed later). The response of the expression of LLT to the PAA- and CHX treatment differs. This finding indicates that the two antisense transcripts are separately regulated. It has been shown that the *llt1* expression is controlled by the LAP (latency-associated promoter), while we assume that the putative antisense promoter (ASP; [13]) controls the expression of *llt2* [112].

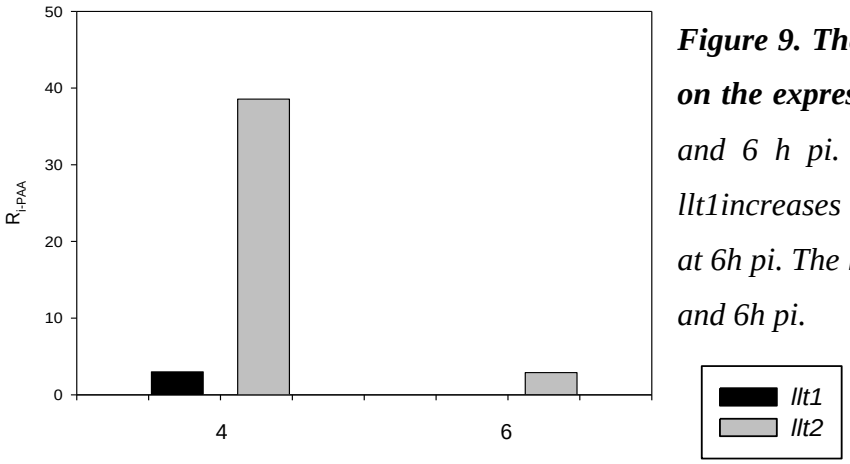

Figure 9. The blocking effect of PAA on the expression of llt1 and llt2 *at 4 and 6 h pi. The expression level of llt1increases at 4h pi, and it decreases at 6h pi. The level of llt2 increases at 4 and 6h pi.*

We detected antisense transcription from the entire PRV genome. For the analysis of AS-RNAs, we also infected the PK-15 cells with high multiplicity of the virus. We categorized these transcripts according to the virus titer and their maximal R value compared to their sense partners. We found that antisense transcripts were expressed at high level in many convergent gene clusters, where the 3'-ends of the oppositely oriented genes located close (within a few hundred bp) to each other. Table 3 shows, the ratios of antisense-sense pairs.

HIGH TITER		R values		Ratio
Gene	Time	mRNAs	AS-RNAs	mRNA/AS-RNA
ep0	8h	4,08	4,31	**1,06**
	12h	1,76	4,40	**2,50**
	18h	1,59	3,51	**2,21**
ul6	12h	1,33	1,60	**1,20**
	18h	0,90	3,01	**3,34**
	24h	1,05	1,97	**1,88**
ul15	12h	0,88	2,15	**2,44**
	18h	0,62	2,79	**4,50**
	24h	0,78	2,77	**3,55**
ul22	18h	0,29	0,68	**2,34**
	24h	0,51	0,98	**1,92**
ul30	4h	0,55	0,65	**1,18**
	6h	0,88	1,77	**2,01**
	8h	0,68	1,91	**2,82**
	12h	1,07	3,15	**2,94**
	18h	1,20	2,80	**2,33**
	24h	1,93	3,81	**1,97**
ul32	1h	0,08	0,11	**1,38**
ul41	8h	0,95	1,70	**1,79**
	12h	2,04	4,31	**2,11**
	18h	1,15	4,10	**3,58**
	24h	2,29	2,46	**1,07**
ul51	6h	1,21	2,16	**1,79**
	18h	3,96	4,92	**1,24**
	24h	3,84	4,16	**1,08**
ul52	6h	1,11	1,19	**1,07**
	8h	1,50	2,67	**1,78**
	12h	3,53	4,92	**1,39**

LOW TITER		R values		Ratio
Gene	Time	mRNAs	AS-RNAs	mRNA/AS-RNA
ep0	2h	0,146	0,180	**1,23**
ul6	1h	0,003	0,217	**72,33**
	2h	0,037	0,188	**5,08**
ul17	2h	0,003	0,008	**2,67**
ul28	6h	0,868	1,293	**1,49**
ul30	6h	0,749	1,075	**1,44**
ul31	1h	0,007	0,009	**1,29**
ul32	1h	0,006	0,006	**1,00**
ul33	2h	0,440	0,490	**1,11**
ul37	1h	0,004	0,004	**1,00**
ul41	1h	0,009	0,016	**1,78**
ul47	1h	0,004	0,019	**4,75**
ul51	1h	0,005	0,013	**2,60**
	4h	0,253	0,323	**1,28**

Table 3. The R values of PRV genes and their antisense partners *in AS-RNAs, which are expressed at a higher level than those of the mRNAs.*

Our results suggest that the oppositely oriented genes exhibit different kinetic properties, while the genes in a nested cluster (3' co-terminal genes) belong to the same kinetic group.

Furthermore, in most cases we found that in the case of two oppositely oriented genes, the expression kinetics of one of the genes coincide with the kinetics of the AS-RNAs produced from the convergent gene, and vice versa. We propose that transcription from one DNA strand negatively influences the expression of the oppositely oriented genes, and that a read-through of transcription across convergent genes is the basis of this regulation. Antisense RNAs may be a result of this putative read-through mechanism [112]. Figure 10 shows the whole PRV genome.

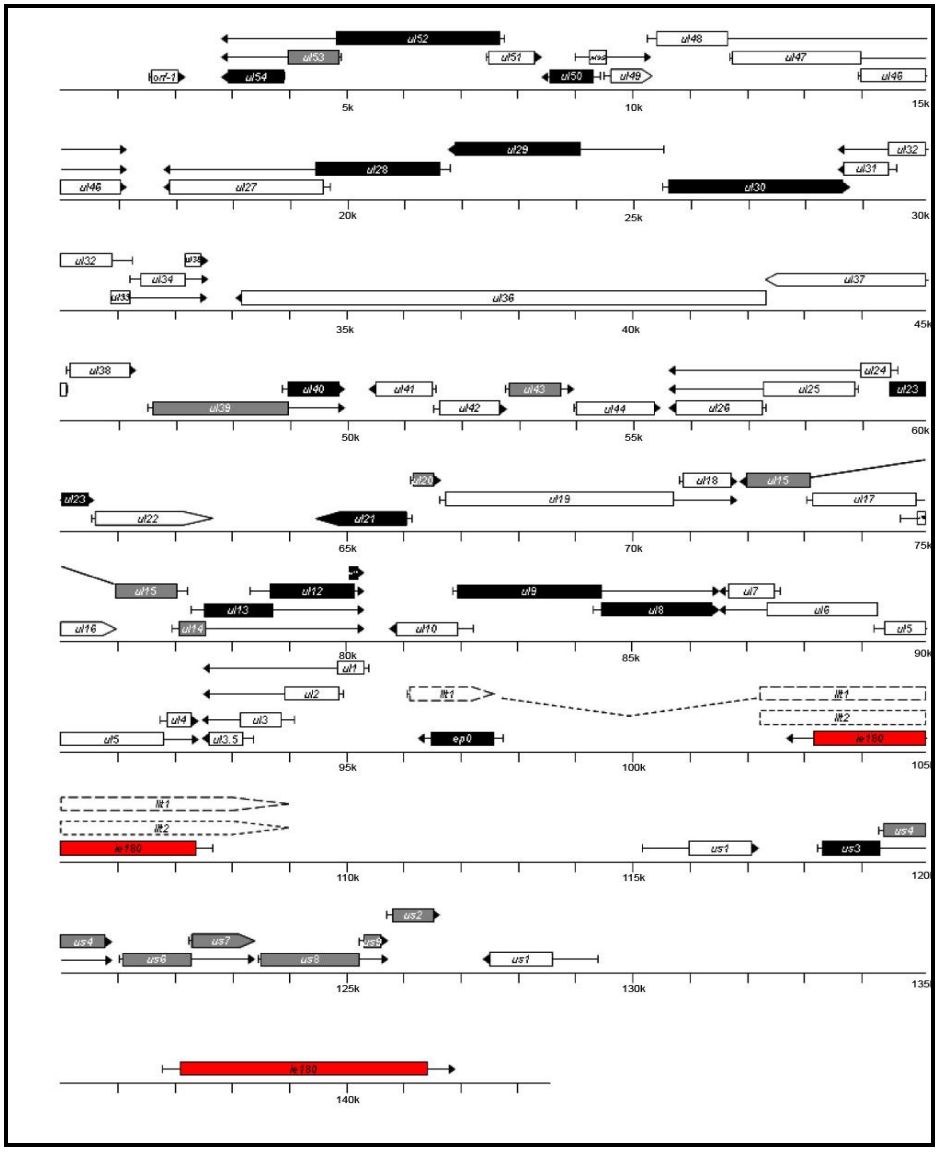

Figure 10. The whole PRV genome *Arrows represent PRV genes and are proportional to lengths of the genes. The kinetic classes of virus genes were determined by PAA analysis. Red indicates IE kinetics, E genes are represented by black, the E/L genes by grey, while the L genes by white color. Dashed arrows are used to indicate the LLT transcripts.*

We found that the *ul30* gene and its AS partner exhibit different expression profiles (Fig 11 A). The *ul30* is an E gene, and it has the highest net increase between 1 and 2h pi. In contrast, its AS-RNA appears to be an L transcript, which shows the highest net increase between the last two time points. Furthermore, this AS-RNA has higher R value at 6h pi, than the mRNA. The *ul31* gene is oppositely oriented to the *ul30* gene and it shows late expression dynamics Figure 11 B shows the running plots of the UL31 transcript and the antisense partner of the *ul31* gene.

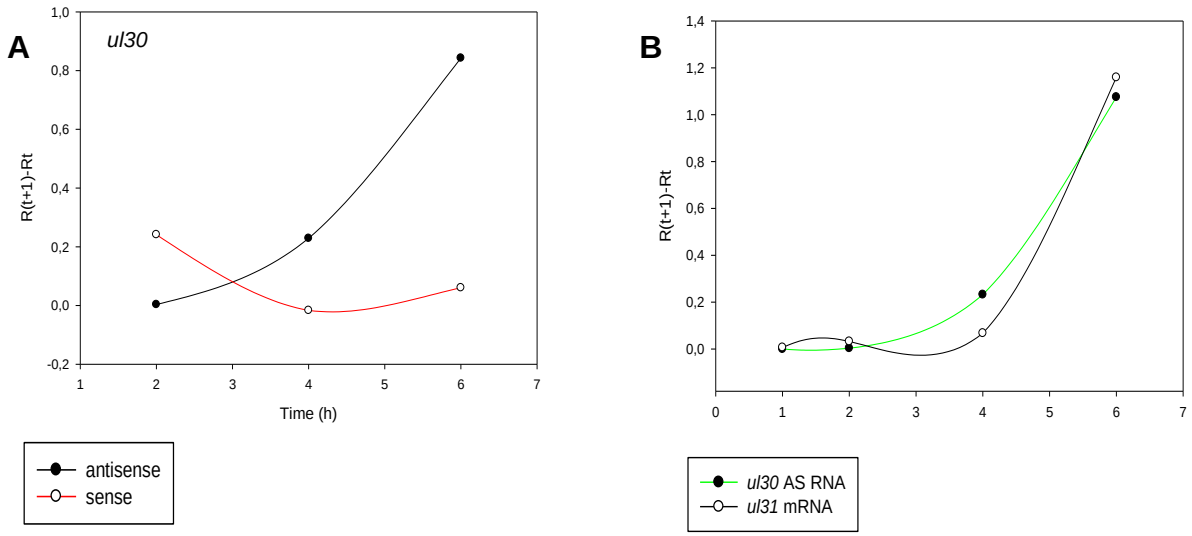

Figure 11. Running curves A. *Running plots of ul30 and its antisense partner using their* R_Δ *values.* ***B.*** *Running plots of the ul31 and the antisense partner of ul30 using their* R_Δ *values.*

We have shown that the expression profiles of the early *ul50* transcript and its AS partner were different, while the mRNA increases between 1-4h pi and it decreases 4-6h, its antisense partner shows continuous increase (Fig 12 A). Furthermore, the expression kinetics of the oppositely oriented *ul51* gene and its AS partner are also different. The protein coding gene is expressed with late kinetics, while the AS-RNA exhibits a significant increase between 1-4 h pi, and it decreases after 4 h (Fig 12 B).

Figure 13 A shows that the AS-RNA of *ul51* and the oppositely oriented *ul50* show the same expression dynamics, as well as the AS partner of *ul50* and the *ul51* gene also exhibit similar, continuous increases during the examined period (Fig. 13 B). We propose that these antisense transcripts are the results of the read-through of the oppositely oriented genes [142-145].

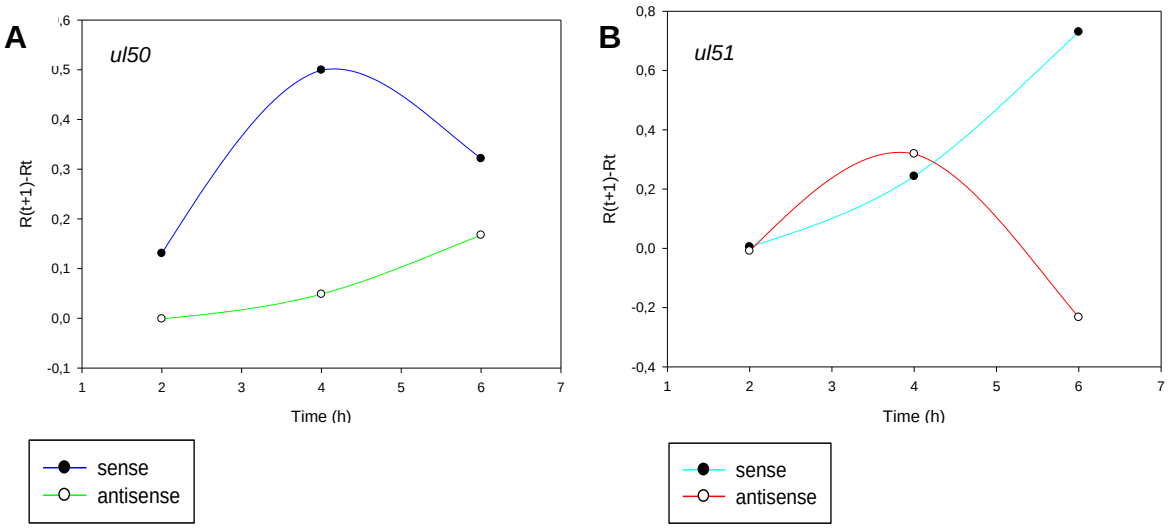

Figure 12. Running plots A*. Running curves of ul50 and its antisense partner are different.* ***B.*** *Running curves of ul51 and its antisense partner.*

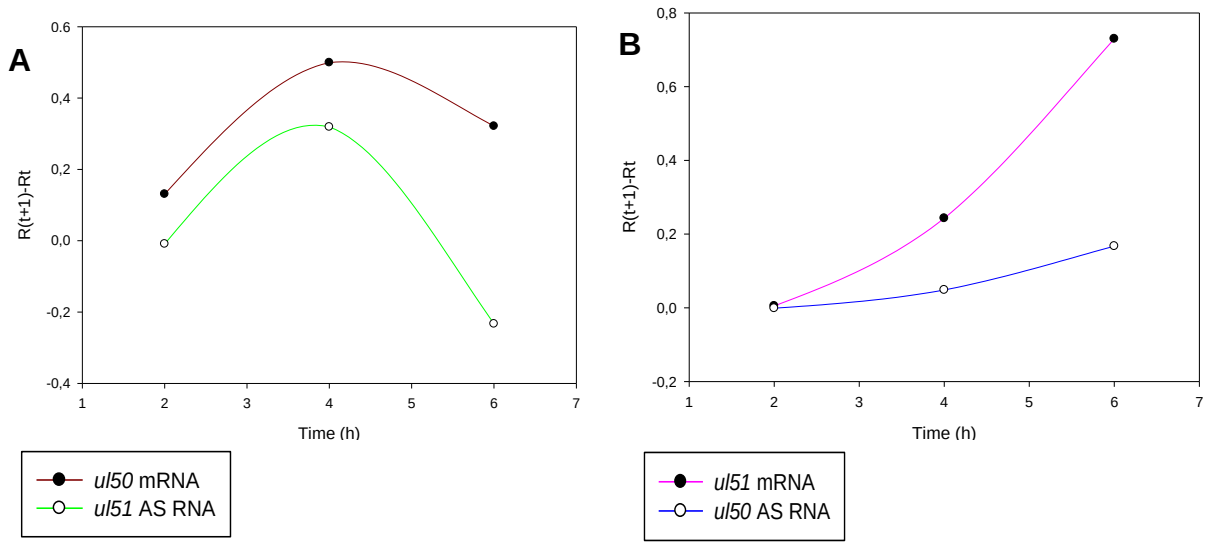

Figure 13. Running curves A. *Running plots of ul50 mRNA and ul51 AS-RNA.****B.*** *Running curves of ul51 mRNA and ul50 AS-RNA.*

Gene expression analysis of a VHS-deleted mutant PRV

We examined the effect of the *vhs* gene on the expression of the other PRV genes. For this, we infected PK-15 cells with *vhs*-mutant Ka PRV. Figure 14 shows a heatmap based on the ratios of the R values of the PRV genes from the *vhs*-deleted and wt virus. Our results show that the VHS protein did not exert inhibitory effect on the expression of PRV genes at 1h pi at all. VHS protein has the highest inhibitory effect on *ep0* gene expression. The difference is 12.8-fold at 12 h pi, 5.1-fold at 6 and 8h pi. We think that the VHS protein has indirect negative effect on the viral mRNAs, by the regulation of the *ep0* gene. Our results revealed that VHS protein has

endonuclease activity on some gene clusters, while mRNA products of other gene groups are not degraded by VHS. VHS did not degrade the mRNAs derived from the "VHS-block" (genes located in the opposite orientation to the *vhs* gene: *ul38*, *ul39*, *ul40*).

In many cases, the expression dynamics of the PRV genes in *vhs*-mutant viruses are delayed compared to the wt PRV genes. Figure 15 shows a heatmap representation of the expression patterns of PRV genes in case of VHS-mutant background. It can be seen that the virus genes show similar expression pattern to each other in VHS-mutant virus. Gene expressions exhibit the highest net increase between 1-2 and/or 2-4h, while they decline between 12-18h [145],

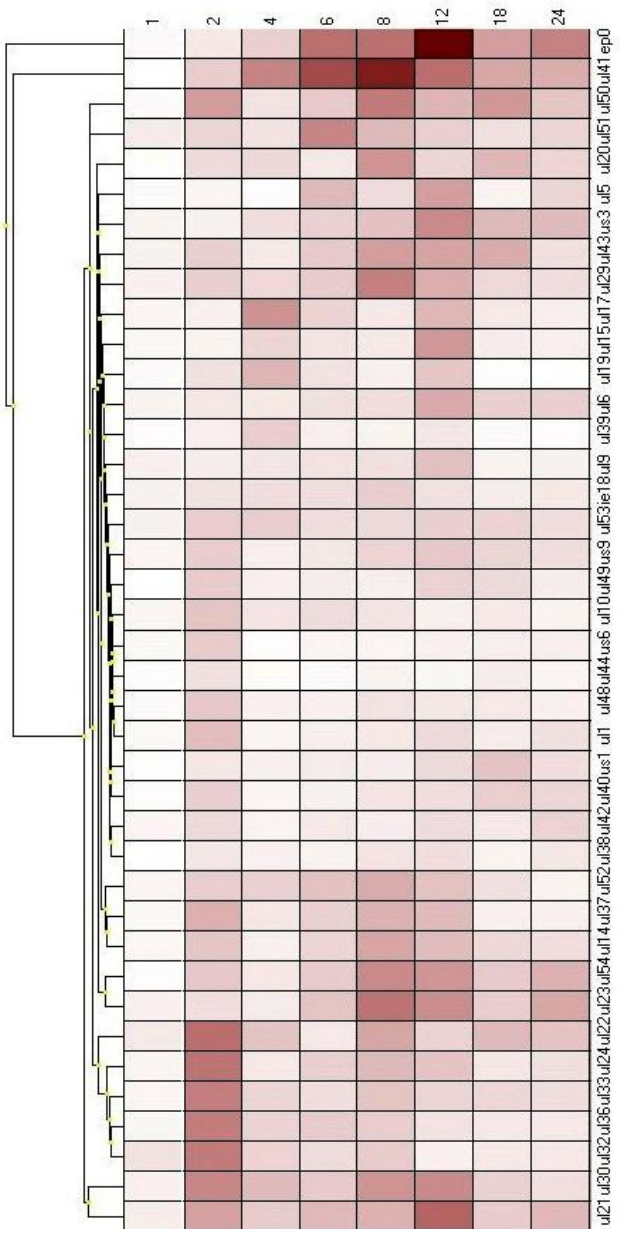

Figure 14. Heatmap of $R_{\Delta VHS}/R_{wt\text{-}PRV}$. *White color indicates the values less than 1, while red color indicates the values which are more than 1. The intensity of the red colors is proportional to the value.*

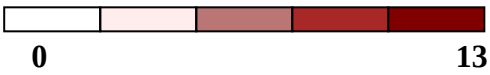

Scale of the ratio of $R_{\Delta VHS}/R_{wt\text{-}PRV}$

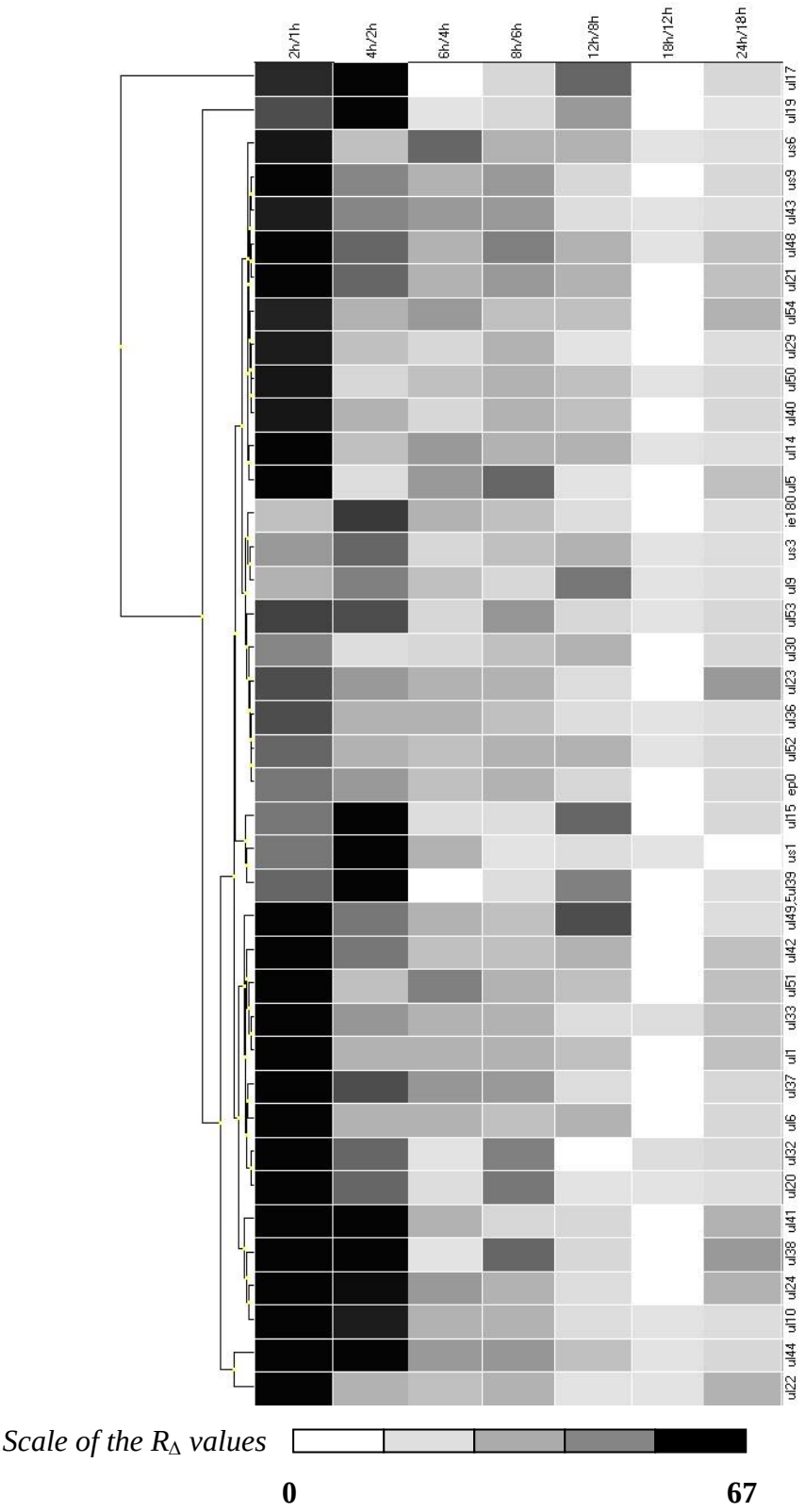

Figure 15. Heatmap of R_Δ values *shows the net increase of the gene expression in VHS-mutant virus. White color represents the R_Δ values when they are less than 1. The intensity of the grey colors is proportional to the R_Δ value. Black color indicates the highest net increase between two time points.*

Analysis of individual PRV genes

The following projects were executed in collaboration with other research groups. Since, I am only a co-author of these works, I summarize the results obtained in this projects more concisely than the results of my first author article. In addition, I primarily focus on the parts of these works what I participated in.

Glycoprotein E and I (gE and gI)

Glycoprotein E and I genes are discussed together here, because they form a heterodimer complex. With the double-deletion of *us8* and *us7* (encoding the glycoprotein E and I, respectively) genes, we generated PRV-ΔgE/gI viruses spreading in an exclusively retrograde manner [6]. To determine if -ΔgE/gI viruses are retrograde transsynaptic tracers, we compared its spreading properties to the well characterized GFP-expressing retrograde PRV152 strain. Similar to PRV152, the injection of As1-PRV08 (Fig. 16.) into the anterior chamber (AntC) of the right eye resulted in retrograde transfer of the virus along the pupillary reflex pathway to the left eye. We detected virus labeling in the Eddinger-Westphal nucleus (EWN), olivary pretectal nucleus (OPN), suprachiasmatic nucleus (SCN), the intergeniculate leaflet (IGL) and the paraventricular nucleus (PVN) of the hypothalamus, however the main targets of retinal ganglion cells, the dorsal lateral geniculate nucleus (dLGN) and the superior colliculus (SC) were free of virus infection [6].

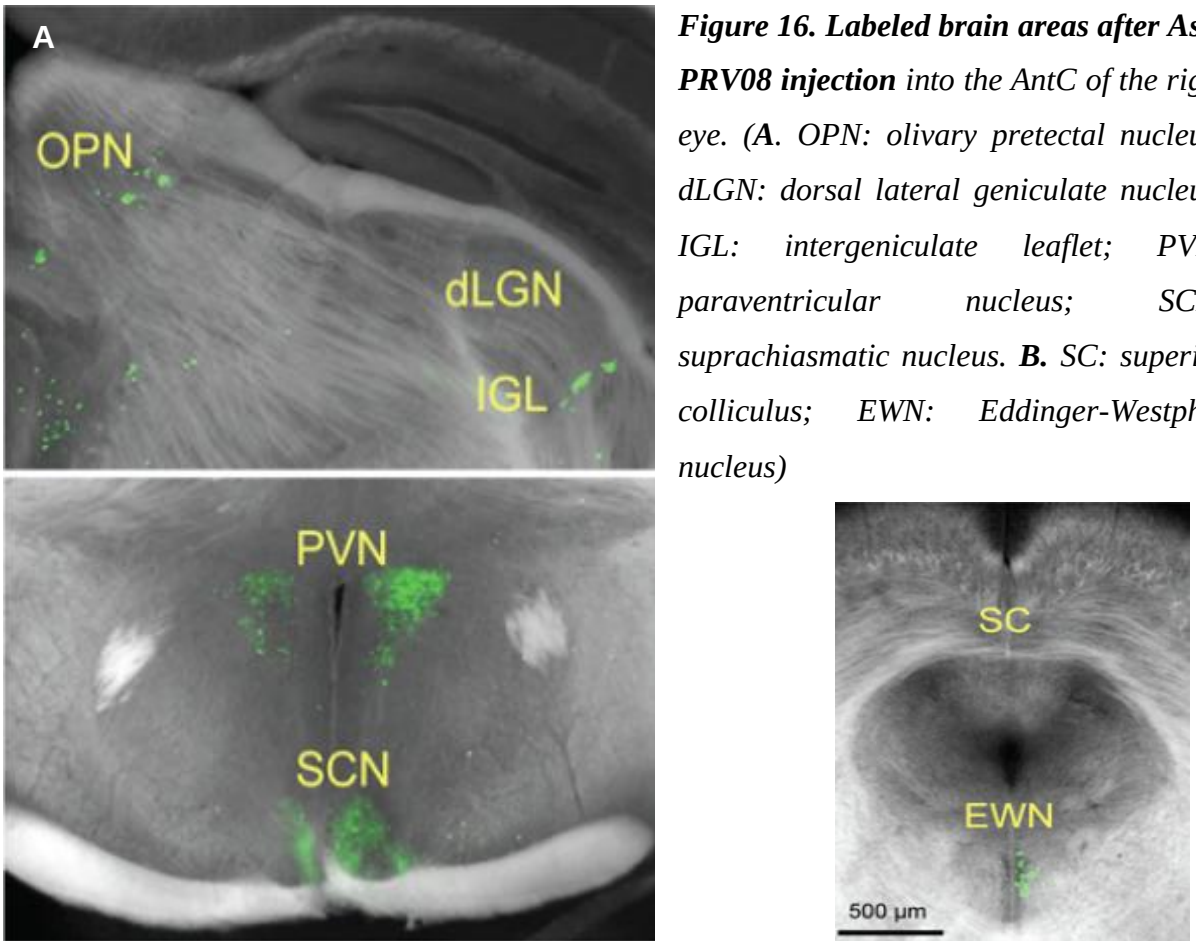

Figure 16. Labeled brain areas after As1-PRV08 injection *into the AntC of the right eye. (**A**. OPN: olivary pretectal nucleus; dLGN: dorsal lateral geniculate nucleus; IGL: intergeniculate leaflet; PVN: paraventricular nucleus; SCN: suprachiasmatic nucleus. **B.** SC: superior colliculus; EWN: Eddinger-Westphal nucleus)*

Thymidine kinase (TK)

Infecting cultured neuron cells with ΔTK PRVs we did not observe cytopathic effects in infected cells (they expressed GFP), which indicates that mutant viruses are non-virulent. [146].

Ribonucleotide reductase (RR)

We have shown that RR-deleted viruses retain their replication properties in cultured cells, but their cytotoxiciy was significantly reduced when infecting non-dividing cardiomyocytes. We observed that the majority of cardiomyocytes retained their normal electrophysiological properties even after three days of infection [9].

Early protein 0 (ep0)

The *ep0* gene is dispensable for viral growth in cell culture, but *ep0* mutant virus produces lower titer and smaller plaques compared to the wt PRVs. Furthermore, we have previously shown that Δ*ep0* viruses are attenuated *in vivo* [34]. Due to these properties Δ*ep0* viruses have been shown to be suitable for gene transfer into cardiomyocytes [9]. The Δ*ep0* strains have also been utilized for tract tracing experiments [6].

Antisense promoter (ASP)

It has been earlier shown in Ba-PRV, that mutation in the ASP region resulted in a significant decrease in virulence of the virus [70]. Our current results show that mutation of this region in the Ka-PRV strain also give rise to a reduced virulence. [6, 9].

The use of genetically modified viruses

A PRV-ΔTK and amplicon-based system for the study of neural connections

We have generated a PRV amplicon-based construct with which we can visualize the presynaptic neurons connected to the infected neurons. Cortical neuronal cultures were co-transfected with a DNA cocktail: amplicon-FP (amp-FP; e.g. amp-memGFP, amp-memCherry or amp-memCerulean) plasmid with a TK-expression cassette and an additional fluorescent protein plasmid, and subsequently infected with the Ba-ΔTK or Ka-ΔgE/gI/TK virus. The TK-defected viruses cannot replicate non-dividing cells, such as neurons. The transfected *tk* expression cassette provides the TK enzyme for the TK-negative virus, therefore, the virus can multiply itself in these cells. However, since the *tk* expression cassette is not integrated to the PRV genome, the viruses can only spread a single synapsis, where it stops due to the lack of TK activity. The amplicons are also incorporated into the virus capsid in productively infected

cells. The amplicon-FP construct was used to allow a discrimination between infection by PRV directly from the culture medium and from a post-synaptic neuron across synapses [146],.

Timer, Rainbow and Activity sensor PRVs for the study of the structure and function of the brain

We have developed fluorescent protein expressing Timer and Rainbow viruses (Fig. 17 A and B) for the study of the neurons and the different brain regions. The Timer viruses express two different fluorescent proteins in a time-shift manner. The primary FP appears at the E stage of infection, while the secondary FP (a soluble reporter) is detectable later. Using these viruses we can gain information about the state of the infection. The Rainbow PRVs express multiple FPs. These viruses facilitate the tracing of several neural networks. We used or the retrograde tracer Bartha PRV or the wt PRV strain that had been engineered to be retrograde by the deletion of the *gE* and *gI* genes of the virus (Ka-ΔgE/gI). The Activity sensor expressing PRVs are suitable tools to report neuronal activity [6],.

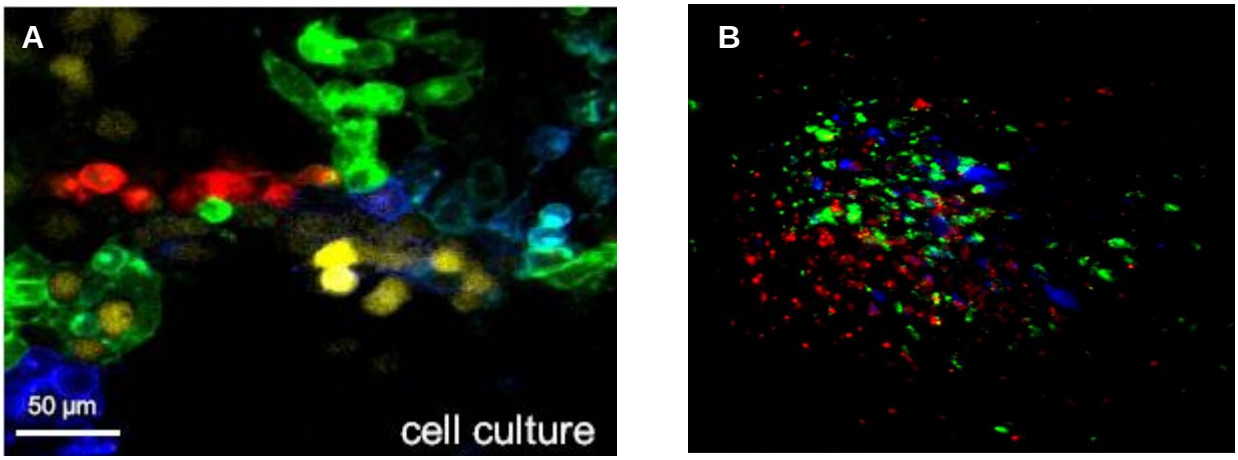

Figure 17. Rainbow viruses A. *Multiple colored, Rainbow viruses in vitro: YFP (dark blue), memCerulean (light blue), memGFP (green) and memCherry (red) in PK-15 cell culture.* ***B.*** *Rainbow PRVs in vitro, in retinal ganglion cells.*

PRV mediated gene delivery to cultured cardiomyocytes

We developed and applied a PRV-based delivery system of a genetically encoded fluorescent Ca^{2+} sensor (troponeon; TN-L15) to adult canine cardiac myocytes. For this, we generated a triple-deletion mutant virus. We deleted the two subunits of the ribonucleotide reductase and the *ep0* encoding genes, and the troponeon was integrated to the TATAA-box of the ASP thereby destroying its function. We showed that the transfer efficiency of troponeon to cultured cardiomyocytes was virtually 100%. Figure 18 shows a schematic representation of

the region of the PRV genome where the modifications have been made. Figure 19 shows the cardiomyocytes after the infection with ΔRR/EP0/ASP – Tropo-PRV [9]

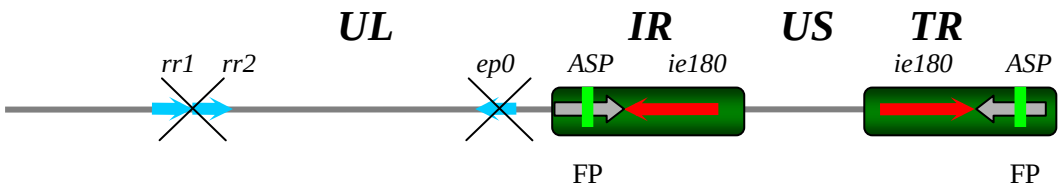

Figure 18. Schematic representation of the ΔRR/EP0/ASP – Tropo-PRV. *(UL: unique long, US: unique short, IR: internal repeat, TR: terminal repeat regions of the virus genome).*

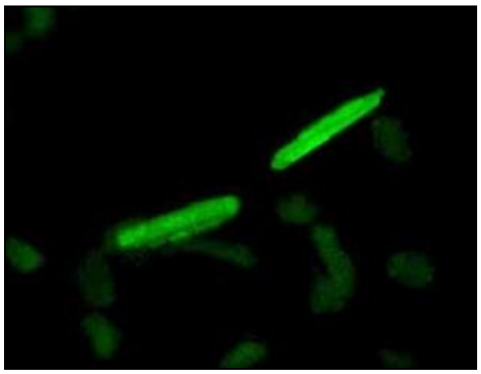

Figure 19. Canine cardiomyocytes *24 hours after infection by troponeon expressing ΔRR/EP0/ASP-PRV.*

Dual viral transneuronal tracing with Ba-DsRed

In this study we have generated a Ba-PRV based mutant virus (Ba-DsRed) via inserting the DsRed reporter gene to the U_L region of the virus located close to the IRS. The growth properties of this mutant virus and Bartha virus were the same in cell culture; they produced the same plaque sizes. The Ba-based mutant virus showed spreading properties similar to those of Bartha virus, indicating that the mutation and the insertion of the transgene did not significantly affect the virulence of the parental virus. In combination with Ba-DupGreen [118], PRV Ba-DsRed proved to be a suitable tool for the separate labeling of ventral lacrimal (SSN) and the dorsal parotid (ISN) groups of salivatory nuclei (Fig 20.).

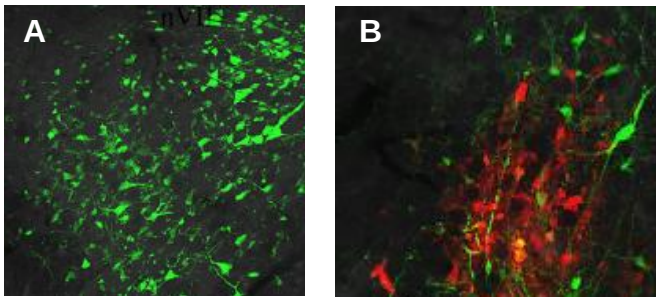

Figure 20. Transneuronal labeling *of the parasympathetic preganglionic neurons of the parotid and lacrimal glands of rat. Fluorescent micrographs of dual-viral-tracing. Green fluorescent protein is expressed in the neurons of the ISN (**A**.) while red fluorescent protein is expressed in the neurons of SSN (**B**.).*

DISCUSSION

Global expression analysis of pseudorabies virus genome

Herpesviruses gene expression have already been studied using traditional (mainly Northern-blot analysis) and also high-throughput techniques (microarray analysis), but because of the limitations of these methods, authors have often categorized the same genes to different kinetic classes. Only partial data are available on the expression of PRV genes. Flori and *coworkers* [30] carried out a whole-genome expression analysis using microarray technique, but they approach did not produce evaluable data on the expression properties of the PRV genes. We employed a novel qRT2-PCR technique using strand-specific primers for the RT to obtain a higher yield and the average maximal E^{Ct} values as the controls for the calculation of relative expression ratios (Rs). Our mathematical approach is a bit complicated, but more accurate than the other known models (Pfaffl-and [119], Souazé-method [120], and the ΔCt and ΔΔCt models [121]). Unlike other models, the variations in the amplification efficiencies of cDNA samples were included in our calculation methods.

Beside the traditional methods, such as PAA (phosphonoacetic acid)- and CHX (cycloheximide) treatment (blockers of DNA replication and *de novo* protein synthesis, respectively) of the virus infected cells, we also analyzed the expression dynamics of the viral genes in untreated samples. Our results conformed well with those published for the HSV genes. The expression level of *ie180* gene was not inhibited by PAA and its expression is even enhanced following CHX treatment. This phenomenon is explained by the fact that the IE180 protein has an inhibitory effect on its own promoter, but this protein is absent in CHX-treated cells, due to blocking the *de novo* protein synthesis by this drug. In principle, the expression of L genes is inhibited by the blockers of the DNA replication, which is not the case of E genes. We categorized the PRV genes to IE, E, E/L and L kinetic groups on the basis of data obtained in untreated an PAA- and CHX- treated samples. The *us1* is an IE gene in the HSV, but in our experiments, it was inhibited by both PAA and CHX, therefore it appeared as an L gene. If the *us1* gene has an important function in the early phase of lytic infection, it might fulfill this without novel protein synthesis by being incorporated in the tegument layer of the virus. The *ul54* and *ep0* gene were shown to be IE genes in HSV, while they show E expression profile in PRV (10, 11), which was confirmed by our experiments.

Our results demonstrate that no apparent sharp boundaries between the E and L gene exist, suggesting that earlier categorization of herpesvirus genes might be arbitrary. The kinetic classes of genes based on our PAA analysis resemble homologous HSV genes more than the

published PRV genes, which can be explained by the semiquantitative methods used for the gene expression analysis of PRV. Our experiments without drug treatment revealed that temporal classification of herpesvirus genes is also possible due to the high sensitivity of the real-time RT-PCR technique. We detected mRNAs in all but 3 PRV genes as early as 1 h pi which indicates that PRV genes are either leaky or subject to regulatory mechanisms which have not yet been elucidated. We found that the expression of E genes are higher than that of L genes at 1, 2 and 4 h pi, as indicated by their higher R values at these time points, and also their R_{Δ} values (net increases) between the 0-1 h, 1-2 h and 2-4 h pi time intervals. However, by the 4-6 h pi period, the L genes exhibited high R_{Δ} values. The classification of the PRV genes through the CHX and PAA analyses led to results very similar those generated by the analysis of untreated cells via the following calculation: R_{Δ}. The differences between the results of the two approaches can be explained by the fact that PAA analysis alone gives only a rough picture of the gene expression; a detailed kinetic analysis of the viral gene expression furnishes a more sophisticated picture. The *ie180* and *us1* genes cannot be classified by PAA-based approach alone.

Analysis of the transcription kinetics of overlapping transcript sets is an important issue. It is not known whether downstream genes on polycistronic mRNAs are translated, and if so, to what extent. This makes interpretation of the mRNA expression data difficult because the mRNA levels cannot be correlated with the amounts of the corresponding proteins, which are the workhorse molecules in regulating cellular physiology. In principle, a downstream gene is translated if it is transcribed from its own promoter. Theoretically, downstream genes could also be translated from a polycistronic RNA if alternative splicing removed upstream gene(s) from the pre-mRNA, or if potential IRES-like sequences helped recruit ribosomes, thereby initiating a cap-independent translation from the downstream gene (we have found no data in the literature concerning these possibilities). Thus, analysis of the downstream genes without discriminating between transcription from their own promoters or by read-through from upstream genes might result in a false categorization.

The PRV genes were also classified by analysis of the gene expression throughout the entire examination period by using Pearson's correlation analysis. Genes with similar expression dynamics (high pairwise Pearson' coefficients) were grouped into the same gene sets. Genes belonging to the same kinetic group (according to our PAA analysis) are generally located in the same gene set generated by the use of Person's correlation; furthermore, members of a particular group rarely display high correlation coefficients with genes belonging in different groups. Based on this analysis, PRV genes were categorized into 10 different gene sets.

We examined the antisense expression from the whole PRV genome. We found that the expression profile of the antisense RNAs from the oppositely oriented gene clusters are inverse, and in many cases the relative copy numbers of these antisense transcripts are higher than its mRNA partners. We found that the the *ep0-llt1* and *ie180-llt2* genes (sense/antisense partners) show inverse expression dynamics. The CHX and PAA analyses revealed an interesting relationship for coordinated regulation of sense/antisense partners. The CHX analysis suggested that IE180 protein inhibits LAP (latency-associated transcript promoter) activity, and facilitates ASP (putative antisense promoter) activity. The PAA treatment resulted in a significantly elevated antisense transcript level at 3 of the 4 time points in LLTs, which indicates the existence of another regulatory layer besides IE180 protein action. We assume that transcription from one DNA strand negatively influences the expression of transcripts from the complementary DNA strand. The interaction can occur at the level of transcription (RNA polymerase moving in one direction along one of the DNA strands inhibits RNA polymerase moving in another direction) and/or translation by forming double-stranded RNAs by the sense and antisense RNAs. As an example, PAA has a negative effect on the transcription of *ie180* (the level of IE180 mRNA is reduced to a quarter) at 4 h pi, which results in a lower rate of transcription from*ie180* (thereby facilitating the expression of LLT2); and a lower amount of inhibitory IE180 proteins, which also facilitates LLT2 expression. Overall, the LLT2 level increases 39.4-fold relative to the untreated conditions. We found that the genes belonging to the oppositely oriented gene clusters show different expression profiles. As well as the AS RNAs have similar expression dynamics as the oppositely oriented genes. Furthermore, genes with the same kinetic properties exhibit a distinctive distribution pattern along the PRV genome. Nested genes appear to belong in the same kinetic class. Additionally, convergent genes and gene clusters in most (3 out of 11) cases belong to different kinetic classes. It is possible that convergent genes grouped to the same kinetic classes might display different expression profiles on a finer scale. The above genome organization principles may point to the existence of yet unknown regulatory mechanisms. It can be speculated as to whether a read-through of transcription across convergent genes is the basis of this regulation. Moreover, groups formed in terms of high Pearson's correlation coefficients contain many genes localized at adjacent loci on the PRV genome. Most genes with high correlation coefficients are not nested genes. This means that the similarity of their expression profiles cannot be explained by the control of a common promoter. Furthermore, several genes in the same group are separated by genes that display different kinetic profiles. These results suggest

the existence of a genetic mechanism that synchronizes gene expression on a higher-order scale.

We have analyzed the effect of VHS mutation on the other PRV genes. Our data revealed that the VHS protein induces endoribonucleolytic activity of certain viral mRNAs. VHS has the highest inhibitory effect on the EP0 expression. We cannot exclude that VHS has an inhibitory effect on the expression of PRV genes through the inhibition of EP0 by degrading the EP0 transcript.

Functional analysis of the virus genes

Timer, Rainbow and Activity sensor viruses for the analysis of the brain structure and function

We used a gE/gIΔ-PRV spreading in a retrograde manner for the generation of Timer, Rainbow and Activity sensor PRVs. Timer viruses express two fluorescent proteins (DsRed2 and GFP) with a delayed expression kinetics to gain information about the state of infection. The multicolored Rainbow PRVs help to dissect the fine structure of brain nuclei sending multiple outputs. Finally, we have developed Activity sensor viruses encoding genetic fluorescent Ca^{2+} sensor to report the activity of the labeled neurons.

This project was executed in cooperation between the Department of Medical Biology, University of Szeged, Szeged, Hungary and the Friedrich Miescher Institute, Basel, Switzerland.

Examination of monosynaptic neural connections

We have generated a four-component system that made it possible to analyze the presynaptic neurons connected to the targeted nerve cells. We deleted the TK gene using as a parental virus, the retrograde tracer Ba-PRV, or the gE/gIΔ-PRV which indicated monosynaptic transsynaptic spreading of the virus. Fluorescent protein expressing PRV-amplicons were used for the visualization of the presynaptic neurons.

These results due to a scientific cooperation with the Medical School, University of Birmingham, Birmingham, United Kingdom.

PRV-mediated gene delivery into cardiomyocytes

Pseudorabies virus is a widely used transsynaptic tracer for the study of neural pathways due to its ability that is to spread across the synapses and deliver marker genes. Tract tracing herpesvirus strains must retain their virulence for their successful spread in the nervous system. However, a gene delivery vector must be non-virulent, otherwise it destroys the physiological functions of the targeted cells. In this study we have developed a herpesvirus-based vector for delivery of genetically encoded activity sensors to cultured canine cardiac myocytes, which is a novel tool in cardiovascular research.

Our system has advantages compare to the earlier applied nonviral methods: we showed that the PRV enters to cells did not cause cytototxic effects, the virus did not change the measured electrophysiological properties of the myocytes for a prolonged period. Cells are suitable for electrophysiological studies after 4 days.

Our results demonstrate that novel PRV-based vectors can transduce genes efficiently into nondividing cardiomyocytes. Thus, PRV can be an alternative to the other viral systems based on adeno-, adeno-associated- and retroviral systems.

This project was performed in cooperation with the Department of Pharmacology and Pharmacotherapy, University of Szeged, Szeged, Hungary.

Dual viral tracing of neurons

We have developed a dual Bartha-PRV-based viral tracer system (Ba-DsRed and Ba-DupGreen), which was utilized for labeling the sensory, the parasympathetic and the sympathetic pathways related to the parotid gland, and for defining the relationship between the ventral lacrimal (SSN) and the dorsal parotid (ISN) groups of salivatory nuclei.

This project was executed in cooperation program with Neuromorphological and Neuroendocrine Research Laboratory, Hungarian Academy of Sciences and Semmelweis University, Budapest, Hungary.

SUMMARY

…OF THE TRANSCRIPTIONAL ANALYSIS

1. We have developed a real-time RT-PCR method for the global analysis of PRV gene expression.
2. We have developed a novel calculation method which allows us to examine the relative expression ratios, characterize the expression dynamics of all PRV genes and also categorized them.
3. This method is applicable to evaluate loss of function phenotypes of mutant viruses and to analyze the antisense transcription from the whole genome.
4. The model is also applicable for the analysis of gene expression in any genetic system that progressively changes in time.

… OF THE VIRAL TRACING METHODS

1. We have developed PRV-based troponeon expressing transsynaptic tracers (activity sensor PRVs) which label synaptically connected nerve cells and also permit assaying the dynamics of activity of neurons located several synapses away from the inoculation site.
2. We have generated timer viruses by inserting a red fluorescent protein gene expression-cassette to the genome of activity sensor PRV. DsRed-2 served as indicator of late phase of virus cycle since it exhibits a slow maturation time, and it was inserted to a transcriptionally less permissive DNA region than the troponeon gene.
3. We have generated Rainbow viruses that are useful for dissecting the local circuit organizations of brain nuclei.
4. We have developed genetically engineered strains of Ba and Ka viruses allowing tracing of presynaptic monosynaptic neuronal connections.
5. We have constructed Ba-DsRed virus which has proved to be an appropriate tool for the study of specific brain regions.

…OF PRV-BASED GENE DELIVERY

1. We have developed a method for short-term culture of isolated canine cardiomyocytes that retains their physiological and morphological integrity and a PRV-based system for delivery of foreign genes to adult cardiac muscle cells.

REFERENCES

1. Ekstrand MI, Enquist LW, Pomeranz LE: The alpha-herpesviruses: molecular pathfinders in nervous system circuits. Trends Mol Med 2008, 14(3):134-40.

2. Aujeszky A: A contagious disease, not readily distinguishable from rabies, with unknown origin. Veterinarius 1902, 25:387-396.

3. Pomeranz LE, Reynolds AE, Hengartner CJ: Molecular biology of pseudorabies virus: impact on neurovirology and veterinary medicine. Microbiol Mol Biol Rev 2005, 69(3):462-500.

4. Enquist LW: Life beyond eradication: veterinary viruses in basic science. Arch Virol 1999, 15:87-109.

5. Card JP, Enquist LW: Transneuronal circuit analysis with pseudorabies viruses. Curr Protoc Neurosci 2001, Chapter 1(Unit 1.5).

6. Boldogkõi Z, Bálint K, Awatramani GB, Balya D, Busskamp V, Viney TJ, Lagali PS, Duebel J, Pásti E, Tombácz D, Tóth JS, Takács IF, Scherf BG, Roska B: Genetically timed, Activity sensor and Rainbow transsynaptic viral tools. Nature Methods 2009, 6:127-130.

7. Granstedt AE, Szpara ML, Kuhn B, Wang SS, Enquist LW: Fluorescence-based monitoring of in vivo neural activity using a circuit-tracing pseudorabies virus. PLoS ONE 2009, 4(9): e6923.

8. Boldogkõi Z, Sík A, Dénes A, Reichart A, Toldi J, Gerendai I, Kovács KJ, Palkovits M: Novel tracing paradigms-genetically engineered herpesviruses as tools for mapping functional circuits within the CNS: present status and future prospects. Prog Neurobiol 2004, 72(6):417-445.

9. Prorok J, Kovács PP, Kristóf AA, Nagy N, Tombácz D, Tóth SJ, Ördög B, Jost N, Virágh L, Papp GJ, Varró A, Tóth A, Boldogkői Z**:** Herpesvirus-mediated delivery of a genetically encoded fluorescent Ca2+ sensor to primary adult canine cardiomyocytes. J Biomed Biotech 2009, 10.1155.

10. Klupp BG Hengartner CJ, Mettenleiter TC, Enquist LW: Complete, annotated sequence of the pseudorabies virus genome. J Virol 2004, 78:424–440.

11. Demarchi JM, Schmidt CA, Kaplan AS: Patterns of Transcription of Human Cytomegalovirus in Permissively Infected Cells. J Virol 1980, 35(2):277-286.

12. Honess RW, Roizman B: Regulation of Herpesvirus Macromolecular Synthesis I. Cascade Regulation of the Synthesis of Three Groups of Viral Proteins. J Virol 1974, 14(1):8-19.

13. Cheung AK: Cloning of the latency gene and the early protein 0 gene of pseudorabies virus. J Virol 1991, 65:5260-5271.

14. Huang C, Wu CY: Characterization and expression of the pseudorabies virus early gene UL54. J Virol Methods 2004, 119:129-136.

15. Fuchs W, Ehrlich C, Klupp BG, Mettenleiter TC: Characterization of the replication origin (Ori(S)) and adjoining parts of the inverted repeat sequences of the pseudorabies virus genome. J Gen Virol 2000, 81:1539-1543.

16. Zhang G, Leader DP: The structure of the pseudorabies virus genome at the end of the inverted repeat sequences proximal to the junction with the short unique region. J Gen Virol 1990, 71:2433-2441.

17. Teri Shors: Understanding Viruses. Sudbury, MA: Jones & Bartlett Publishers; 2008.

18. Hann LE, Cook WJ, Uprichard SL, Knipe DM, Coen DM: The role of herpes simplex virus ICP27 in the regulation of UL24 gene expression by differential polyadenylation. J Virol 1998, 72(10):7709-7714.

19. Pearson A, Knipe DM, Coen DM: ICP27 selectively regulates the cytoplasmic localization of a subset of viral transcripts in herpes simplex virus type 1-infected cells. J Virol 2004, 78(1):23-32.

20. Chambers J, Angulo A, Amaratunga D, Guo H, Jiang Y et al: DNA microarrays of the complex human cytomegalovirus genome: profiling kinetic class with drug sensitivity of viral gene expression. J Virol 1999, 73(7):5757-5766.

21. Stingley SW, Ramirez JJ, Aguilar SA, Simmen K, Sandri-Goldin RM, Ghazal P, Wagner EK: Global analysis of herpes simplex virus type 1 transcription using an oligonucleotide-based DNA microarray. J Virol 2000, 74(21):9916-9927.

22. Kennedy PG, Grinfeld E, Craigon M, Vierlinger K, Roy D, Forster T, Ghazal P: Transcriptomal analysis of varicella-zoster virus infection using long oligonucleotide-based microarrays. J Gen Virol 2005, 86(10):2673-2684.

23. Aguilar JS, Devi-Rao GV, Rice MK, Sunabe J, Ghazal P, Wagner EK: Quantitative comparison of the HSV-1 and HSV-2 transcriptomes using DNA microarray analysis. Virol 2006, 348(1):233-241.

24. Yang WC, Devi-Rao GV, Ghazal P, Wagner EK, Triezenberg SJ: General and specific alterations in programming of global viral gene expression during infection by VP16 activation-deficient mutants of herpes simplex virus type 1. J Virol 2002, 76(24):12758-74.

25. Sun A, Devi-Rao GV, Rice MK, Gary LW, Bloom DC, Sandri-Goldin RM, Ghazal P, Wagner EK: Immediate-early expression of the herpes simplex virus type 1 ICP27 transcript is not critical for efficient replication in vitro or in vivo. J Virol 2004, 78(19):10470-10478.

26. Karaca G, Hargett D, McLean TI, Aguilar JS, Ghazal P, Wagner EK, Bachenheimer SL: Inhibition of the stress-activated kinase, p38, does not affect the virus transcriptional program of herpes simplex virus type 1. Virol 2004, 329(1):142-156.

27. Blanchard Y, Le MN, Le CM, Blanchard P, Leger J, Jestin A: Cellular gene expression survey of PseudoRabies Virus (PRV) infected Human Embryonic Kidney cells (HEK-293). Vet Res 2006, 37:705-723.

28. Brukman A, Enquist LW: Suppression of the interferon-mediated innate immune response by pseudorabies virus. J Virol 2006, 80:6345-6356.

29. Ray N, Enquist LW: Transcriptional response of a common permissive cell type to infection by two diverse alphaherpesviruses. J Virol 2004, 78:3489-3501.

30. Flori L, Rogel_Gaillard C, Cochet M, Lemonnier G, Hugot K, Chardon P, Robin S, Lefèvre F: Transcriptomic analysis of the dialogue between Pseudorabies virus and porcine epithelial cells during infection. BMC Genomics 2008, 9:123.

31. Øster B, Bundgaard B, Höllsberg P: Viral gene expression patterns in human herpesvirus 6B-infected T cells. J Virol 2002, 76(15):7578-7586.

32. Dittmer DP, Gonzalez CM, Vahrson W, DeWire SM, Hines-Boykin R, Damania : Whole-genome transcription profiling of rhesus monkey rhadinovirus. J Virol 2005, 79(13):8637-8650.

33. Cheung, AK, Fang JJ, Wesley RD: Characterization of a pseudorabies virus that is defective in the early protein 0 and latency genes. Am J Vet Res 1994, 55:1710-1716.

34. Boldogkoi Z, Braun A, Fodor I: Replication and virulence of early protein 0 and long latency transcript deficient mutants of the Aujeszky's disease (pseudorabies) virus. Microbes Infect 2000, 2:1321–1328.

35. Davison AJ: Evolution of the herpesviruses. Vet Microbiol 2002, 86:69–88.

36. Del Rio T, Decoste CJ, Enquist LW: Actin is a component of the compensation mechanism in pseudorabies virus virions lacking the major tegument protein VP22. J Virol 2005, 79:8614–8619.

37. Mettenleiter TC: Herpesvirus Assembly and Egress. J Virol. 2002. 76(4): 1537–1547.

38. Sydiskis RJ, Roizman B: Polysomes and protein synthesis in cells infected with a DNA virus. Science 1966, 1;153(731):76-8.

39. Zelus BD, Stewart RS, Ross J: The virion host shutoff protein of herpes simplex virus type 1: messenger ribonucleolytic activity in vitro. J Virol 1996, ;70(4):2411-9.

40. Everly DN Jr, Read GS: Site-directed mutagenesis of the virion host shutoff gene (UL41) of herpes simplex virus (HSV): analysis of functional differences between HSV type 1 (HSV-1) and HSV-2 alleles. J Virol 1999, 73(11):9117-29.

41. Smith TJ, Ackland-Berglund CE, Leib DA: Herpes simplex virus virion host shutoff (vhs) activity alters periocular disease in mice. J Virol 2000, 74(8):3598-604.

42. Oroskar AA, Read GS: Control of mRNA stability by the virion host shutoff function of herpes simplex virus. J Virol 1989, 63(5):1897-906.

43. Strelow LI, Leib DA: Role of the virion host shutoff (vhs) of herpes simplex virus type 1 in latency and pathogenesis. J Virol 1995, 69(11):6779-86.

44. Nishioka Y, Silverstein S: Degradation of cellular mRNA during infection by herpes simplex virus. PNAS 1977, 74(6):2370-4.

45. Suzutani T, Nagamine M, Shibaki T, Ogasawara M, et al: The role of the UL41 gene of herpes simplex virus type 1 in evasion of non-specific host defence mechanisms during primary infection. J Gen Virol 2000, 81(Pt 7):1763-71.

46. Read GS, Karr BM, Knight K: Isolation of a herpes simplex virus type 1 mutant with a deletion in the virion host shutoff gene and identification of multiple forms of the vhs (UL41) polypeptide. J Virol 1993, 67(12):7149-60.

47. Schmelter J, Knez J, Smiley JR, Capone JP: Identification and characterization of a small modular domain in the herpes simplex virus host shutoff protein sufficient for interaction with VP16. J Virol 1996, 70(4):2124-31.

48. Strelow LI, Leib DA: Analysis of conserved domains of UL41 of herpes simplex virus type 1 in virion host shutoff and pathogenesis. J Virol 1996, 70(8):5665-7.

49. Strelow L, Smith T, Leib D: The virion host shutoff function of herpes simplex virus type 1 plays a role in corneal invasion and functions independently of the cell cycle. Virol 1997 28;231(1):28-34.

50. Mettenleiter TC: Aujeszky's disease (pseudorabies) virus: the virus and molecular pathogenesis–state of the art, June 1999. Vet Res 2000, 31:99–115.

51. Mettenleiter TC: Immunobiology of pseudorabies (Aujeszky's disease).Vet Immunol Immunopathol 1996, 54:221–229.

52. Tyborowska J, Reszka N, Kochan G, Szewczky B: Formation of pseudorabies virus glycoprotein E/I complex in baculovirus recombinant system. Acta virol 2006, 50:169-174.

53. Mettenleiter TC: Herpesvirus assembly and egress. J Virol 2002, 76: 1537–1547.

54. Whealy ME, Card JP, Robbins AK, Dubin JR, Rhiza HJ, Enquist L: Specific pseudorabies virus infection of the rat visual system requires both gI and gp63 glycoproteins. J Virol 1993, 67:3786-97.

55. Mettenleiter TC, Lukacs N, Rziha HJ: Mapping of the Structural Gene of Pseudorabies Virus Glycoprotein A and Identification of Two Non-Glycosylated Precursor Polypeptides. J Virol 1985, 53:52-57.

56. Some Genetic Functions Encoded by Herpes Simplex Virus type 1**:**
http://darwin.bio.uci.edu/~faculty/wagner/table.html

57. The Genetic and Transcription Map of the HSV-1 Genome **:**
http://darwin.bio.uci.edu/~faculty/wagner/hsvimg04z.jpg

58. Roizman B: The function of herpes simplex virus genes: A primer for genetic engineering of novel vectors. PNAS 1996, 93:11307-11312

59. Roizman B, Campadelli-Fiume G: Alphaherpes viral genes and their functions. In Human Herpesviruses - Biology, Therapy and Immunoprophylaxis. Edited by: Arvin A, et al. Cambridge: Cambridge University Press; 2007:70-92.

60. Kritas SK, Pensaert MB, Mettenleiter TC: Invasion and spread of single glycoprotein deleted mutants of Aujeszky's disease virus (ADV) in the trigeminal nervous pathway of pigs after intranasal inoculation. Vet Microbiol 1994, 40:323-34.

61. Kritas SK, Pensaert MB, Mettenleiter TC: Role of envelope glycoproteins gI, gp63 and gIII in the invasion and spread of Aujeszky's disease virus in the olfactory nervous pathway of the pig. J Gen Virol 1994, 75:2319-27.

62. Kimman D, de Wind TGN, Oei-Lie N, Pol JM, Berns AJ, Gielkens AL: Contribution of single genes within the unique short region of Aujeszky's disease virus (suid herpesvirus type 1) to virulence, pathogenesis and immunogenicity. Vet Microbiol 1992, 33:45-52.

63. Babic E, Klupp B, Brack A, Mettenleiter TC, Ugolini G, Flamand A: Deletion of glycoprotein gE reduces the propagation of pseudorabies virus in the nervous system of mice after intranasal inoculation. Virol 1996, 219:279-84.

64. Tirabassi RS, Townley RA, Eldridge MG, Enquist LW: Characterization of Pseudorabies Virus Mutants Expressing Carboxy-Terminal Truncations of gE : Evidence for Envelope Incorporation, Virulence and Neurotropism Domains. J Virol 1997, 71:6455-6464.

65. Fuchs W, Klupp BG, Granzow H, Hengartner C, Brack A, Mundt A, Enquist LW, Mettenleiter TC: Physical interaction between envelope glycoproteins E and M of pseudorabies virus and the major tegument protein UL49. J Virol 2002, 76:8208-17.

66. Zsak L, Mettenleiter TC, Sugg N, Ben-Porat T: Release of pseudorabies virus from infected cells is controlled by several viral functions and is modulated by cellular components. J Virol 1989, 63:5475-5477.

67. Husak PJ, Kuo T, Equist LW: Pseudorabies Virus Membrane Proteins gI and gE Facilitate Anterograde Spread of Infection in Projection - Specific Neurons in the Rat. J Virol 2000, 74(23):10975–10983.

68. Kit S, Kit M,. Pirtle EC: Attenuated properties of thymidine kinase-negative deletion mutant of pseudorabies virus. Am J Vet Res 1985, 46:1359-1367

69. McGregor S, Easterday BC, Kaplan AS, Ben-Porat T: Vaccination of swine with thymidine kinase-deficient mutants of pseudorabies virus. Am J Vet Res 1985, 46:1494-1497.

70. de Wind N, Berns A, Gielkens A, Kimman T: Ribonucleotide reductase-deficient mutants of pseudorabies virus are avirulent for pigs and induce partial protective immunity. J Gen Virol 1993, 74:351-359.

71. Boldogkői Z, Reichart A, Tóth IE, Sík A, Erdélyi F et al: Construction of recombinant pseudorabies viruses optimized for labeling and neurochemical characterization of neural circuitry. Mol Brain Res 2002, 109 (1-2): 105-118.

72. Kwong AD, Frenkel N: The herpes simplex virus virion host shutoff function. J Virol 1989, 63: 4834-4839.

73. Ladin BF, Blankenship ML, Ben-Porat T: Replication of herpesvirus DNA. V. Maturation of concatemeric DNA of pseudorabies virus to genome length is related to capsid formation. J Virol 1980, 33:1151-1164.

74. Wu CA, Harper L, Ben-Porat T: Molecular basis for interference of defective interfering particles of pseudorabies virus with replication of standard virus. J Virol 1986, 59:308-317.

75. Zhang G, Raghavan B, Kotur M, Cheatham J, Sedmak D et al: Antisense transcription in the human cytomegalovirus transcriptome. J Virol 2007, 81 (20): 11267-81.

76. Johnson C, Sundaresan V: Regulatory small RNAs in plants Plant. Systems Biol 2007, 97:99-113.

77. Sanna CR, Li WH, Zhang L: Overlapping genes in the human and mouse genomes. BMC Genomics 2008, 14(9):169.

78. Mattick JS: Deconstructing the Dogma: A New View of the Evolution and Genetic Programming of Complex Organisms. Annals of the New York Academy of Sciences 2009, 1178(1): 29-46(18).

79. Jin H, Vacic V, Girke T, Lonardi S, Zhu JK: Small RNAs and the regulation of cis-natural antisense transcripts in Arabidopsis. BMC Mol Biol 2008, 14;9:6.

80. Anderson S, Bankier AT, Barrell BG, de Bruijn MHL, Coulson AR et al: Sequence and organization of the human mitochondrial genome. Nature 1981, 290, 457 – 465.

81. Boi S, Solda G, TenchiniML: Shedding light on the dark side of the genome: overlapping genes in higher eukaryotes. Curr Genomics 2004, 5, 509–524.

82. Wang XJ, Gaasterland T, Chua NH: Genome-wide prediction and identification of cis-natural antisense transcripts in Arabidopsis thaliana. Genome Biol 2005, 6:R30

83. Katayama S, Tomaru Y, Kasukawa T, Waki K, Nakanishi M, et al.: Antisense Transcription in the Mammalian Transcriptome. Science 2005, 309: 5740, 1564 – 1566.

84. Carninci P, Kasukawa T, Katayama J, Gough J, Frith MC, et al.: The Transcriptional Landscape of the Mammalian Genome. Science 2005, 309: 5740, 1559-1563

85. Cheng J, Kapranov P, Drenkow J, Dike S, Brubaker S et al.: Transcriptional maps of 10 human chromosomes at 5-nucleotide resolution. Science 2005, 20;308(5725):1149-54

86. He H, Wang J, Liu T, Liu XS, Li T et al: Mapping the *C. elegans* noncoding transcriptome with a whole-genome tiling microarray, Genome Res 2007, 17:1471-1477.

87. Nagalakshmi U, Wang Z, Waern K, Shou C, Raha D et al: The transcriptional landscape of the yeast genome defined by RNA sequencing. Science 2007, 316(5830):1484-8.

88. Kapranov P, Cheng J, Dike S, Nix DA, Duttagupta R et al: RNA Maps Reveal New RNA Classes and a Possible Function for Pervasive Transcription. Science 2007, 8;316:1484-8.

89. Wagner EG, Simons RW: AntisenseRNAcontrol in bacteria, phages, and plasmids. Annu Rev Microbiol 1994, 48: 713–742.

90. Vanhée-Brossollet C, Vaquero C: Do natural antisense transcripts make sense in eukaryotes? Gene 1998, 211(1):1-9.

91. Mattick JS, Amaral PP, Dinger ME, Mercer TR, Mehler MF: RNA regulation of epigenetic processes. Bioessays 2009, 31(1):51-9.

92. Chamberlain SJ, Brannan CI: The Prader-Willi syndrome imprinting center activates the paternally expressed murine Ube3a antisense transcript but represses paternal Ube3a. Genomics 2001, 73(3):316-22.

93. Taft RJ, Pang KC, Mercer TR, Dinger M, Mattick JS: Non-coding RNAs: regulators of disease. J Pathol 2009, 220(2):126-139.

94. Tam OH, Aravin AA, Stein P, Girard A, Murchison EP et al: Pseudogene-derived small interfering RNAs regulate gene expression in mouse oocytes. Nature 2008, 453, 534-538

95. Borsani O, Zhu J, Verslues PE, Sunkar R, Zhu JK: Endogenous siRNAs derived from a pair of natural cis-antisense transcripts regulate salt tolerance in Arabidopsis. Cell 2005, 123(7):1279-91.

96. Watanabe T, Totoki Y, Toyoda A, Kaneda M, Kuramochi-Miyagawa S et al: Endogenous siRNAs from naturally formed dsRNAs regulate transcripts in mouse oocytes. Nature 2008, 453, 539-543.

97. Okamura K, Chung WJ, Ruby JG, Guo H, Bartel DP, Lai EC: The Drosophila hairpin RNA pathway generates endogenous short interfering RNAs. Nature 2008, 453, 803-806.

98. Zamore PD, Haley B: Ribo-gnome: The Big World of Small RNAs. Science 2005, 309(5740):1519–1524.

99. Jacquemont B, Roizman B: RNA synthesis in cells infected with herpes simplex virus. X. Properties of viral symmetric transcripts and of double-stranded RNA prepared from them. J Virol. 1975, 15(4):707-13.

100. Bohenzky RA, Lagunoff M, Roizman B, Wagner EK, Silverstein S: Two overlapping transcription units which extend across the L-S junction of herpes simplex virus type 1. J Virol 1995, 69:2889–2897.

101. Borchers K, Wolfinger U, Lawrenz B, Schellenbach A, Ludwig H: Equine herpesvirus 4 DNA in trigeminal ganglia of naturally infected horses detected by direct in situ PCR. J Gen Virol 1997, 78:1109–1114.

102. Carter KL, Ward PL, Roizman B: Characterization of the products of the U(L)43 gene of herpes simplex virus 1: potential implications for regulation of gene expression by antisense transcription. J Virol 1996, 70: 7663–7668.

103. Cheung AK:. The BamHI J fragment (0.706 to 0.737 map units) of pseudorabies virus is transcriptionally active during viral replication. J Virol 1990, 64:977–983.

104. Wirth UV, Vogt B, Schwyzer M: The three major immediateearly transcripts of bovine herpesvirus 1 arise from 2 divergent and spliced transcription units. J Virol 1991, 65:195–205.

105. Basua K, Gravel C, Tomioka R, Kaneko T, Tamamaki N, Sík A: Novel strategy to selectively label excitatory and inhibitory neurons in the cerebral cortex of mice. J Neurosci Meth 2008, 170:2 212-219.

106. Weiss P, Hiscoe HN: Experiments on the mechanism of nerve growth. 1948. J Exp Zool 107, 315–395.

107. Rothermel M, Schöbel N, Damann N, Klupp BG et al: Anterograde transsynaptic tracing in the murine somatosensory system using Pseudorabies virus (PrV): A “live-cell”-tracing tool for analysis of identified neurons in vitro. J Neurovirol 2007, 13. 6: 579-585

108. Enquist LW, Cardy JP: Recent advances in the use of neurotropic viruses for circuit analysis. Curr Opinion Neurobiol 2003, 13:603–606.

109. Bartha A: Experimental reduction of virulence of Aujesky's disease virus. Magyar Állatorvosok Lapja 1961, 16:42-45.

110. Lomniczi B, Watanabe S, Ben-Porat T, Kaplan AS: Genome location and identification of functions defective in the Bartha vaccine strain of pseudorabies virus. J Virol 1987, 61:796-801.

111. Lyman MG, Demmin GL, Banfield BW: The attenuated pseudorabies virus strain Bartha fails to package the tegument proteins Us3 and VP22. J Virol 2003, 77:1403-1414.

112. Tombácz D, Tóth JS, Petrovszki P, Boldogkői Z: Whole-genome analysis of pseudorabies virus gene expression by real-time quantitative RT-PCR assay. BMC Genomics 2009, 10:491

113. Rezek Ö, Boldogkői Z, Tombácz D**,** Kővágó C, Gerendai I, Palkovits M, Tóth IE: Location of parotid preganglionic neurons in the inferior salivatory nucleus and its relation to the superior salivatory nucleus of rat. Transneuronal labeling by pseudorabies viruses. Neurosci Lett 2008, 440(3): 265-269.

114. Papin J, Vahrson W, Hines-Boykin R, Dittmer DP: Real-time quantitative PCR analysis of viral transcription. Methods Mol Biol 2005, 292:449-480.

115. Soong R, Tabiti K: Detection of colorectal micrometastasis by quantitative RT-PCR of cytokeratin 20 mRNA. Proceedings of the American Association for Cancer Research 2000, 41:391.

116. Elhai J, Wolk CP: A versatile class of positive-selection vectors based on the nonviability of palindrome-containing plasmids that allows cloning into long polylinkers. Gene 1988, 68(1):119-138.

117. Heim N, Griesbeck O: Genetically encoded indicators of cellular calcium dynamics based on troponin C and green fluorescent protein. J Biol Chem 2004, 279(14):14280–14286.

118. Tóth IE, Wiesel O, Boldogkői Z, Bálint K, Tapaszti Z, Gerendai I: Predominance of supraspinal innervation of the left ovary. Microsc Res Technol 2007, 70: 710–718.

119. Pfaffl MW: A new mathematical model for relative quantification in real-time RT-PCR. Nucleic Acids Res 2001, 29(9)**:**e45.

120. Souazé F, Ntodou-Thomé A, Tran CY, Rostène W, Forgez P: Quantitative RT-PCR: limits and accuracy. Biotechniques 1996, 21(2)**:**280-285.

121. Livak KJ, Schmittgen TD: Analysis of relative gene expression data using real-time quantitative PCR and the 2ΔΔ C(T) Method. Methods 2001, 25(4)**:**402-408.

122. Gómez-Sebastián S, Tabarés E**:** Negative regulation of herpes simplex virus type 1 ICP4 promoter by IE180 protein of pseudorabies virus. J Gen Virol 2004, 85:2125-2130.

123. Fuchs W, Klupp BG, Granzow H, Osterrieder N, Mettenleiter TC: The Interacting UL31 and UL34 Gene Products of Pseudorabies Virus Are Involved in Egress from the Host-Cell Nucleus and Represent Components of Primary Enveloped but Not Mature Virions. J Virol 2002, 76(1):364-378.

124. Bras F, Dezelee S, Simonet B, Nguyen X et al: The left border of the genomic inversion of pseudorabies virus contains genes homologous to the UL46 and UL47 genes of herpes simplex virus type 1, but no UL45 gene. Virus Res 1999, 60:29-40.

125. Reynolds AE, Fan Y, Baines JD: Characterization of the UL33 gene product of herpes simplex virus 1. Virology 2000, 266:310-8.

126. McNabb DS, Courtney RJ: Identification and characterization of the herpes simplex virus type 1 virion protein encoded by the UL35 open reading frame. J Virol 1992, 66:2653-63.

127. Klupp BG, Fuchs W, Granzow H et al: Pseudorabies virus UL36 tegument protein physically interacts with the UL37 protein. J Virol 2002, 76:3065-3071.

128. Braun A, Kaliman A, Boldogkõi Z, Aszódi A, Fodor I: Sequence and expression analyses of the UL37 and UL38 genes of Aujeszky's disease virus. Acta Vet Hung 2000, 48(1):125-136.

129. Ambagala AP, Hinkley S, Srikumaran S: An early pseudorabies virus protein down-regulates porcine MHC class I expression by inhibition of transporter associated with antigen processing (TAP). J Immunol 2000, 164:93-99.

130. Powers L, Wilkinson KS, Ryan P: Characterization of the prv43 gene of pseudorabies virus and demonstration that it is not required for virus growth in cell culture. Virol 1994, 199:81-88.

131. Robbins AK, Watson RJ, Whealy ME, Hays WW, Enquist LW: Characterization of a pseudorabies virus glycoprotein gene with homology to herpes simplex virus type 1 and type 2 glycoprotein. J Virol 1986, 58(2):339-347.

132. Kaelin K, Dezelee S, Masse MJ, Bras F, Flamand A: The UL25 Protein of Pseudorabies Virus Associates with Capsids and Localizes to the Nucleus and to Microtubules. J Virol 2000, 74:474-482.

133. Dezélée S, Bras F, Vende P, Simonet B, Nguyen X, Flamand A, Masse MJ: The BamHI fragment 9 of pseudorabies virus contains genes homologous to the UL24, UL25, UL26, and UL 26.5 genes of herpes simplex virus type 1. Virus Res 1996, 42:27-39.

134. Yamada S, Imada T, Watanabe W, Honda Y et al: Nucleotide sequence and transcriptional mapping of the major capsid protein gene of pseudorabies virus. Virology 1991, 185:56-66.

135. Dijkstra JM, Fuchs W, Mettenleiter TC, Klupp BG: Identification and transcriptional analysis of pseudorabies virus UL6 to UL12 genes. Arch Virol 1997, 142:17-35.

136. 55 Dean HJ, Cheung AK: A 3'coterminal gene cluster in pseudorabies virus contains herpes simplex virus UL1, UL2, UL3 gene homologs and a unique UL3.5 open reading frame. J Virol 1993, 67:5955-5961.

137. Krause PR, Croen KD, Ostrove JM, Straus SE: Structural and Kinetic Analyses of Herpes Simplex Virus Type I Latencyassociated Transcripts in Human Trigeminal Ganglia and in Cell Culture. J Clin Invest 1990, 86(1):235-241.

138. van Zijl M, Gulden H, de Wind N, Gielkens A, Anton Berns A: Identification of Two Genes in the Unique Short Region of Pseudorabies Virus; Comparison with Herpes Simplex Virus and Varicella-zoster Virus. J Gen Virol 1990, 71:1747-1755.

139. de Wind N, Peeters B et al: Mutagenesis and characterization of a 41-kilobase-pair region of the pseudorabies virus genome: transcription map, search for virulence genes, and comparison with homologs of herpes simplex virus type 1. Virology 1994, 200:784-790.

140. Dean HJ, Cheung AK: Identification of the pseudorabies virus UL4 and UL5 (helicase) genes. Virology 1994, 202(2):962-7.

141. Van Minnebruggen G, Favoreel HW, Jacobs L, Nauwynck HJ: Pseudorabies virus US3 protein kinase mediates actin stress fiber brakedown. J Virol 2003, 77(16):9074-80.

142. Tombácz D, Boldogkői Z: Az Aujeszky-féle vírus összgenom analízise Real-Time RT-PCR-ral. VIII. Genetikai minikonferencia, 2009, Szeged, Hungary

143. Tombácz D, Tóth JS, Boldogkői Z: Whole-genome analysis of pseudorabies virus by Real-Time RT-PCR. 2nd CEFORM Central European Forum for Microbiology, 2009, Keszthely, Hungary

144. Tombácz D, Tóth JS, Takács IF, Boldogkői Z: Global analysis of pseudorabies virus gene expression by RT-PCR. Advances In Genomics Symposium, 2010, Ghent, Belgium

145. Tombácz D, Tóth JS, Petrovszki P, Boldogkői Z: Real-time RT-PCR Profiling of Global mRNA Transcription from Pseudorabies Virus Genome. 34th International Herpesvirus Workshop, 2009, Ithaca, NY, USA

146. Ferecskó AS, Boldogkői Z, Tombácz D, Ördög B, Hirase H, Tiesinga P, Sík A: Development of a novel pseudorabies virus-based method for monosynaptic neuronal network tracing. IBRO International Workshop, 2010, Pécs, Hungary

ACKNOWLEDGEMENTS

I am especially grateful to my supervisor Professor Zsolt Boldogkői for his scientific guidance, encouragement, support and friendship he gave me.

I thank to the former and present members of Boldogkői's research team.

I am very thankful to the colleagues in the Department of Medical Biology.

This work was supported by Hungarian National Fund for Scientific Research (OTKA T049171), Human Frontiers Science Program Young Investigator Grant to Zsolt Boldogkői (RGY0073/2006) and PhD Program of the University of Szeged.